NASA TECHNICAL NOTE

NASA TN D-8199

NASA TN D-8199

RESULTS OF SOIL MOISTURE FLIGHTS DURING APRIL 1974

Thomas J. Schmugge, Bruce J. Blanchard, William J. Burke, Jack F. Paris, and James R. Wang

Goddard Space Flight Center
Greenbelt, Md. 20771

NATIONAL AERONAUTICS AND SPACE ADMINISTRATION • WASHINGTON, D. C. • MAY 1976

1. Report No.	2. Government Accession No.	3. Recipient's Catalog No.
TN D-8199		

4. Title and Subtitle

Results of Soil Moisture Flights During April 1974

5. Report Date: May 1976

6. Performing Organization Code: 913

7. Author(s): T. Schmugge, B. Blanchard, W. Burke, J. Paris, and J. Wang

8. Performing Organization Report No.: G-7663

9. Performing Organization Name and Address

Goddard Space Flight Center
Greenbelt, Maryland 20771

10. Work Unit No.: 177-51-41

11. Contract or Grant No.

13. Type of Report and Period Covered: Technical Note

12. Sponsoring Agency Name and Address

National Aeronautics and Space Administration
Washington, D.C. 20546

14. Sponsoring Agency Code

15. Supplementary Notes

16. Abstract

The results presented here are derived from measurements made during the April 5 and 6, 1974 flights of the NASA P-3A aircraft over the Phoenix, Arizona agricultural test site. The purpose of the mission was to study the use of microwave techniques for the remote sensing of soil moisture. These results include infrared (10- to 12-μm) 2.8-cm and 21-cm brightness temperatures for approximately 90 bare fields. These brightness temperatures are compared with surface measurements of the soil moisture made at the time of the overflights. These data indicate that the combination of the sum and difference of the vertically and the horizontally polarized brightness temperatures yield information on both the soil moisture and surface roughness conditions.

17. Key Words (Selected by Author(s))	18. Distribution Statement
Remote sensing, Soil moistures, Microwave radiometers	Unclassified—Unlimited CAT. 43

19. Security Classif. (of this report)	20. Security Classif. (of this page)	21. No. of Pages	22. Price*
Unclassified	Unclassified	57	$4.25

For sale by the National Technical Information Service, Springfield, Virginia 22161

This document makes use of international metric units according to the Systeme International d'Unites (SI). In certain cases, utility requires the retention of other systems of units in addition to the SI units. The conventional units stated in parentheses following the computed SI equivalents are the basis of the measurements and calculations reported.

CONTENTS

RESULTS OF SOIL MOISTURE FLIGHTS DURING APRIL 1974

Thomas J. Schmugge
Goddard Space Flight Center

Bruce J. Blanchard*
Texas A&M University

William J. Burke†
Johnson Space Center

Jack F. Paris‡
University of Houston

James R. Wang
Computer Sciences Corporation

INTRODUCTION

There has been a continuing need for soil moisture information for large areas in the following disciplines:

- Hydrology—for the partioning of rainfall into runoff, deep percolation, and storage;
- Meteorology—for the estimation of the moisture and heat fluxes into the atmosphere from land surfaces; and
- Agriculture—for the estimation crop productivity.

Therefore, the development of a technique for the remote sensing of soil moisture over large areas would be very beneficial. One of the most promising techniques uses microwave sensors because of the large difference in the dielectric properties of water and those of dry soils at microwave wavelengths. As a result, the dielectric properties of soils are strongly dependent on their moisture content. Field measurements (Poe et al., 1971) on smooth, bare fields indicated the sensitivity of microwave brightness temperature to soil moisture variations. Experiments performed from aircraft platforms (Schmugge et al., 1974) have verified that microwave radiometers could remotely sense soil moisture

*Formerly with USDA/Agricultural Research Service, Chickasha, Oklahoma.

†National Academy of Science Postdoctoral Research Associate.

‡Formerly with Lockheed Electronics Company, Inc., Houston, Texas.

variations. However, there was a considerable amount of scatter in the data which has been attributed to the differing degrees of surface roughness, different soil types, and uncertainties in the vertical distribution of moisture in the soil. Thus, more work was needed to quantify these effects. To accomplish this, a group of scientists working on the problem met in August 1973 at the Johnson Space Center (JSC) to develop a program combining laboratory, field, and aircraft experiments. These investigators came from NASA, the Agricultural Research Service of USDA, the Environmental Research Institute of Michigan (ERIM), the University of Arkansas, the University of Kansas, and Texas A&M University. This cooperative effort has been called the Joint Soil Moisture Experiment (JSME).

The first aircraft experiment occurred in April 1974 over the irrigated agricultural area in the vicinity of Phoenix, Arizona. It involved the NASA P-3A aircraft carrying microwave radiometers and the ERIM C-46 carrying synthetic aperture radars (SAR). This report is an analysis of the microwave radiometer results. The radar results are analyzed elsewhere (Cihlar et al., 1975).

The use of microwave radiometers for soil moisture sensing has also been studied by scientists in the USSR (Basharinov et al., 1974). Under the auspices of the Joint US/USSR Working Group on the Natural Environment, a program for coordinated research in the microwave sensing of soil moisture has been agreed to by the two countries. A major part of the agreement provided for flights with airborne microwave radiometers over selected test sites in the two countries. The mission described in this report was conducted as a part of the agreement.

EXPERIMENTAL PROCEDURES AND APPARATUS

The first aircraft flight mission studying the use of microwave radiometers for the remote sensing of soil moisture conducted by the JSME group was over an irrigated agricultural area near Phoenix, Arizona. The flights, flown by the NASA P-3A aircraft, were on the afternoon of April 5 and at dawn on April 6, 1974. The aircraft altitude for these flights was 700 to 800 m; the ground speed was 82 m/s (160 knots). Meteorological conditions were clear at the time of both flights. The air temperature was between 301 and 303 K (28 and 30°C) for the afternoon flight and was 286 K (13°C) for the dawn flight.

Experience from previous experiments has shown that the physically significant parameters for radiometric detection of soil moisture are:

- Frequency of radiation,
- Polarization of radiation,
- Look angle of the detectors,
- Soil texture,
- Soil moisture profile,
- Soil temperature profile,

- Surface roughness, and
- Vegetative cover.

While the first three are under the experimenter's control, the last few are given by nature. The aircraft and ground truth aspects of the experiment were designed to measure all of the parameters but the last. This parameter was excluded for the time being by studying only bare fields.

The aircraft had two microwave radiometers on board: (1) a dual polarized, scanning X-band (2.8-cm) radiometer with half power beam width of 2.6° by 1.6° at a constant nadir look angle of 49° and (2) a nonscanning L-band (21-cm) radiometer with a half power beam width of 15° which views the surface at a nadir look angle fixed by the experimenter. In this flight the nadir look angles were set at 0° and 40°. Because the antenna measures only one polarization at a time, it was necessary to make three runs over the flight lines. On the first run the antenna viewed the nadir scene; vertical and horizontal polarizations at a look angle of 40° were observed on runs 2 and 3. Predawn data were acquired for the nadir look angle. The aircraft also carried a scanning (uncalibrated) and a nonscanning (calibrated) infrared radiometer both operating in the 10 to 12 μm band, which were used to provide surface temperature information. Photographic coverage was obtained to verify the aircraft's flight path.

Ground measurements of the soil moisture and temperature profiles as well as surface roughness photographs were obtained for approximately 100 bare 400- by 400-m (40-acre) fields. These 100 fields were distributed along 4 flight lines: 2 north-south lines west of the city and 2 east-west lines south of the city. The flight lines were chosen to fly over pairs of these fields. The microwave brightness temperatures were determined for about 40 pairs at 21 cm and for all the fields at 2.8 cm. A detailed description of the flight lines and the field characteristics is included in Appendix A. The coordinates of the aircraft flight lines as well as the sense in which the aircraft flew for various L-band antenna configurations are found in table 1.

The predawn flight was undertaken to study the diurnal variation of both the microwave and infrared brightness temperatures. The diurnal range of surface temperatures has been shown to be a good indicator of soil moisture (Idso et al., 1975). The flight was scheduled for first light so that the aircraft pilot could follow the correct paths and before the rising sun could significantly perturb nighttime surface conditions.

Ground-Based Observations

This section summarizes the ground truth effort provided in support of the Phoenix experiment. The Phoenix site was selected for several reasons. First, it had been studied previously by Schmugge et al. (1974); secondly, the fields are regularly set along straight lines; thirdly, the agriculture is on irrigated land. During early April, a large number of bare fields were either planted in cotton or being prepared for planting, and therefore we expected to observe a wide variety of soil moisture conditions. However, this, for the most part, was not observed.

Table 1
Coordinates of Aircraft Flight Tracks

Line	South End	North End	Pass 1 Nadir	Pass 2 Vertical Polarization	Pass 3 Horizontal Polarization	Pass 4 Nadir
1	33°20.7'N	33°38.0'N	11:51 - 11:55	12:53 - 12:59	13:30 - 13:36	5:55 - 6:02
	112°15.0'W	112°15.0'W	S→N	N→S	S→N	
2	33°20.7'N	33°38.0'N	12:00 - 12:08	12:42 - 12:49	13:47 - 13:54	6:04 - 6:11
	112°15.5'W	112°15.5'W	N→S	S→N	N→S	
	West End	East End				
3	33°22.0'N	33°22.0'N	12:19 - 12:23	13:15 - 13:20	14:03 - 14:08	6:13 - 6:23
	112°00.0'W	111°35.0'W	W→E	E→W	W→E	
4	33°21.6'N	33°21.6'N	12:28 - 12:33	13:07 - 13:13	14:10 - 14:15	6:29 - 6:40
	112°00.0'W	111°35.0'W	E→W	W→E	E→W	

The soil moisture profiles of each field were estimated by taking soil samples from the top and bottom of furrows at four separated points marked 1, 2, 3, and 4 of the map (Appendix A). At each point, samples were taken from layers from 0 to 1, 1 to 2, 2 to 5, 5 to 9, and 9 to 15 cm. Thus, a total of 40 moisture samples per field were obtained. The samples were taken to a USDA laboratory where they were weighed, baked for 24 hours at 378 K (105°C), and reweighed to determine the percentage of moisture by weight. The average value of the percentage of moisture found in each of the five layers is given in table 2.

The reliability of our sampling procedure was tested by sampling a moderately wet field, 260B, from line 4 (Appendix A), at 36 locations from the top and the bottom of the furrows. Figure 1 illustrates the contours of soil moisture in the 0- to 1-cm layer of the bottom (figure 1a) and the top (figure 1b) of the furrows. These figures indicate that drying rates vary considerably within a field. An estimate of the accuracy of the four-point data set was obtained by dividing the field into four groups of nine locations. One hundred stratified random samples consisting of one sample for each quarter of the field were selected. The means of the stratified random samples were calculated and compared to the overall mean of the field. The distribution of means from the sets of four random locations were not normally distributed about the field mean. The distribution of the 100 means for each depth indicates that there is a 90 percent chance that the sample from four locations in the field will fall within the following limits:

Depth (cm)	Mean (%)	Limits (%)
0-1	15.8	-2.9 to 3.5
1-2	18.4	-2.6 to 3.1

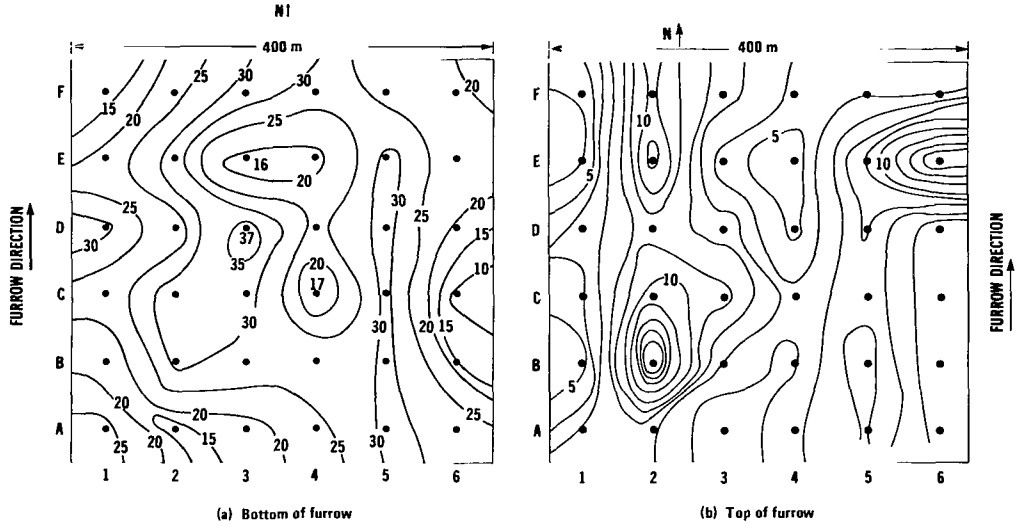

Figure 1. Soil moisture contours for the 0- to 1-cm layer of soil for field 260B.

2-5	21.8	-2.5 to 2.4
5-9	23.1	-1.8 to 2.6
9-15	23.9	-1.5 to 1.7

A more comprehensive summary of the ground truth selection criteria and sampling reliability is given in Appendix B.

On completion of the second weighing procedure, a texture analysis was performed on the soils to determine the relative mixtures of sand, silt, and clay particles. The results of these analyses are found in the last three columns of table 2.

The temperature profiles of the soils were measured using cylindrical probes with embedded thermocouples placed at the center of the five layers. The results of these measurements are given in table 2. A note of caution should be introduced in using these data. While the three runs of the afternoon flight went from 1150 to 1415 MST, the ground data were collected between 1100 and 1730 MST. The average value and standard deviation of the temperatures measured in the top centimeter of soil during a given half hour are given in figure 2. These data indicate a tendency for the temperature of the top centimeter to rise at a rate of ~1.3 K/hr between 1100 and 1500 MST. After this time the soil cools.

As a measure of the surface roughness, a set of three photographs was taken in each field against the background of a gridded panel. One picture had the grid crossing the furrows. The other two were taken with the grid along the tops and bottoms of the furrows. Because of the relatively uniform cultivation practices of Phoenix farmers, only three types of large scale roughness were recorded: (1) listed fields with a mean height of furrows of 27 cm at a separation of 1 m; (2) planted fields with a mean furrow height of ~5 cm separated by ~30 cm; and (3) flat fields. Examples of listed and planted fields are given in figures 3a and 3b. The only flat field was field 317. The direction of the

Table 2
Soil Moisture and Temperature for April 5, 1974

Field Number	Percentage of Moisture by Weight					Temperature of Soil °C*					Texture		
	0-1 cm	1-2 cm	2-5 cm	5-9 cm	9-15 cm	0-1 cm	1-2 cm	2-5 cm	5-9 cm	9-15 cm	Sand	Silt	Clay
11	2.27	3.99	11.77	17.70	18.21	34.2	32.7	30.7	26.6	21.3	55	21	24
12	1.70	3.69	9.14	12.05	11.65	37.7	35.9	33.0	27.8	22.3	56	23	21
13	4.46	5.89	9.06	12.16	13.77	33.1	31.9	29.9	24.7	19.1	55	21	24
14	1.38	2.23	6.03	10.54	11.16	37.2	35.7	32.9	27.1	21.2	56	23	21
38	1.55	2.38	9.32	15.03	15.79	33.9	33.5	31.3	27.4	22.4	52	20	28
39	1.75	1.97	15.17	16.09	16.98	37.0	36.5	35.0	30.7	22.8	50	23	27
42	1.30	2.86	11.58	15.47	16.16	36.4	35.1	33.0	29.3	24.2	48	26	26
43	1.08	1.72	8.66	12.59	12.78	36.3	34.5	31.4	27.5	22.5	62	18	20
51A	1.65	2.77	6.78	9.56	9.95	38.1	37.3	35.5	30.7	25.3	51	19	30
51B	1.85	2.82	4.82	8.19	10.88	39.1	38.3	36.4	31.9	24.5	47	16	37
60A	15.10	17.30	20.87	22.06	22.35	33.0	31.7	29.9	26.3	21.1	48	20	32
60B	1.40	2.81	5.87	13.34	14.94	35.8	35.4	34.8	32.5	26.9	52	23	25
61A	1.98	4.90	14.22	17.63	17.76	32.5	30.7	28.1	22.8	18.8	46	22	32
62B	3.09	8.59	19.32	20.91	21.25	35.1	33.3	30.5	25.8	20.5	28	34	38
99A	2.71	7.62	20.72	21.81	23.30	36.8	35.7	33.5	28.7	21.1	25	40	35
99B	3.20	12.33	21.30	22.90	23.32	36.2	34.5	32.1	27.6	20.4	17	44	39
103A	3.32	6.36	18.88	19.94	20.90	35.2	34.0	32.4	28.3	21.7	20	45	35
104A	3.81	7.96	23.24	24.34	24.51	33.0	31.7	30.0	26.7	21.5	12	44	44
104B	3.58	12.78	21.34	23.77	24.55	33.0	31.0	29.1	25.8	21.0	15	40	45
105A	2.34	6.15	19.53	22.59	24.59	34.3	31.8	28.6	22.5	18.3	17	41	42
105B	2.45	6.51	18.90	22.37	23.77	33.8	31.9	30.5	24.2	18.1	17	41	42
106A	27.09	31.62	32.58	30.34	30.07	30.1	29.0	27.7	24.9	21.5	18	39	43
106B	6.73	12.98	20.68	24.45	26.06	30.9	29.8	28.1	25.4	21.8	17	42	41
106C	5.10	14.66	25.52	28.26	28.17	0.0	0.0	0.0	0.0	0.0	18	39	43
107A	2.76	6.58	12.41	17.83	20.11	36.0	33.8	31.1	25.5	20.4	17	40	43
107B	5.62	10.18	17.66	25.21	26.37	33.4	30.9	28.0	22.8	18.3	20	37	43
121A	1.20	2.39	12.07	15.64	16.33	35.0	32.7	31.7	27.1	21.0	46	30	24
121B	1.78	5.12	12.23	16.71	24.64	34.0	31.8	29.0	25.0	20.5	45	28	27
127	1.66	2.84	9.98	16.35	19.43	32.4	30.3	27.3	22.3	18.0	41	25	34

*Add 273.2 to convert to K.

Table 2 (Continued)

Field Number	Percentage of Moisture by Weight					Temperature of Soil °C*					Texture		
	0-1 cm	1-2 cm	2-5 cm	5-9 cm	9-15 cm	0-1 cm	1-2 cm	2-5 cm	5-9 cm	9-15 cm	Sand	Silt	Clay
131	1.39	2.50	8.92	15.86	19.25	32.2	31.2	29.6	23.9	18.3	42	25	33
132	1.74	3.28	9.43	16.40	18.25	32.1	30.3	27.9	23.1	17.3	44	26	30
237A	3.33	4.44	11.60	14.90	17.47	32.3	33.1	34.3	26.1	20.7	31	24	45
237B	1.16	2.85	10.36	15.57	17.55	23.8	23.2	22.5	20.1	18.8	47	18	35
242A	1.94	4.42	10.15	13.32	15.90	30.1	27.9	25.9	21.7	18.7	47	18	35
242B	1.68	3.47	8.20	13.54	16.30	34.1	31.8	28.8	22.9	18.3	42	21	37
243A	2.86	5.40	9.17	15.44	17.80	31.4	29.5	26.9	21.0	15.2	44	20	36
243B	1.54	2.77	6.83	13.60	17.50	35.0	32.4	29.6	23.7	19.0	44	20	36
248A	6.73	8.46	14.56	20.30	22.63	30.3	28.9	27.2	23.7	20.3	32	19	49
248B	4.47	8.52	13.83	19.35	22.37	31.0	29.5	28.1	24.7	20.4	32	22	46
249A	2.32	5.82	15.47	22.82	22.94	33.3	31.7	29.8	25.2	20.5	22	25	53
249B	1.90	5.25	15.32	22.42	23.07	32.4	30.9	28.6	23.9	20.0	25	23	52
252A	1.53	3.24	10.82	16.57	19.34	36.1	34.1	31.9	26.7	21.2	41	23	36
252B	1.74	3.98	12.26	18.04	19.74	35.1	33.7	31.6	26.3	21.7	28	28	44
254	4.16	7.26	17.23	22.78	24.16	32.4	30.6	27.7	22.7	16.8	30	18	52
255	3.40	7.12	17.43	21.92	23.99	33.8	31.5	27.8	22.0	17.1	35	16	49
257	3.35	7.64	17.16	22.32	22.99	35.1	33.5	30.7	24.9	18.4	33	16	51
260A	10.13	14.50	21.68	28.55	24.59	31.9	29.8	27.3	23.3	16.8	39	17	44
260B	13.73	17.60	22.34	23.20	25.16	32.4	30.8	28.5	25.6	16.3	38	16	46
260C	4.96	11.86	17.43	19.73	20.55	0.0	0.0	0.0	0.0	0.0	39	17	44
260D	8.82	15.94	22.22	22.96	23.94	0.0	0.0	0.0	0.0	0.0	38	16	46
261A	3.84	9.17	18.71	20.29	20.43	31.9	31.4	28.7	24.1	17.3	47	15	38
261B	3.49	8.28	15.96	18.08	17.95	35.6	34.1	32.3	28.0	20.4	38	19	43
284A	3.10	6.69	15.36	18.35	19.30	36.5	34.6	31.9	27.0	20.1	51	15	34
264B	1.79	3.95	13.07	16.57	18.93	37.0	34.8	31.8	26.2	18.8	46	12	42
264C	3.04	5.43	14.28	17.67	18.46	37.2	35.7	33.6	29.4	22.0	59	12	29
264D	2.00	4.65	11.98	15.19	18.35	36.1	34.3	31.7	27.3	21.1	58	13	29
297A	2.20	4.27	10.55	15.15	16.83	33.0	31.7	29.1	24.2	18.8	60	13	27
297B	2.86	5.69	12.61	16.16	17.41	32.9	31.1	28.4	23.5	18.8	53	16	31
299	4.13	7.86	15.60	18.34	20.00	34.6	33.3	30.7	25.7	19.6	58	10	32
300	3.28	8.08	16.13	17.94	19.25	30.8	29.2	27.1	22.6	17.1	59	8	33

*Add 273.2 to convert to K.

Table 2 (Continued)

Field Number	Percentage of Moisture by Weight					Temperature of Soil °C*					Texture		
	0-1 cm	1-2 cm	2-5 cm	5-9 cm	9-15 cm	0-1 cm	1-2 cm	2-5 cm	5-9 cm	9-15 cm	Sand	Silt	Clay
315A	1.75	4.43	14.77	18.00	18.58	39.2	38.0	33.7	26.3	19.3	48	16	36
315B	2.03	7.84	15.03	16.28	17.45	37.9	36.5	33.5	27.7	20.3	59	16	25
316A	2.14	5.69	12.06	17.29	19.49	39.0	38.9	38.1	35.5	29.4	44	23	33
316B	1.28	3.08	13.36	14.77	14.44	38.5	37.1	33.3	26.6	20.6	57	15	28
316C	1.30	1.96	4.57	11.94	15.87	32.0	29.6	25.7	19.7	14.0	60	14	26
316D	1.13	2.00	11.56	13.67	13.98	34.1	32.0	29.6	25.2	20.9	65	16	19
317A	2.09	3.17	6.49	10.54	13.25	28.5	26.9	24.6	21.1	18.1	55	18	27
318A	1.08	1.84	7.98	13.33	14.74	32.2	30.2	27.0	22.2	15.7	52	23	25
318B	1.52	2.68	11.29	13.16	13.59	34.8	33.1	29.9	25.3	21.1	65	17	18
319A	10.86	13.71	17.28	18.18	18.93	0.0	0.0	0.0	0.0	0.0	68	18	14
319B	11.02	16.13	17.09	16.61	18.18	0.0	0.0	0.0	0.0	0.0	58	18	24
319C	2.57	5.46	14.32	16.86	18.45	34.4	33.2	30.9	25.5	16.1	68	18	14
319D	4.37	9.52	12.64	16.63	18.52	35.3	34.4	32.7	28.6	18.5	58	18	24
333A	1.58	2.94	4.92	8.43	9.61	29.6	27.1	26.7	24.2	17.9	70	17	13
333B	1.62	2.05	5.31	9.85	10.98	34.3	33.9	33.3	31.7	24.2	62	20	18
334A	1.85	2.11	8.52	13.31	14.23	36.9	35.9	34.3	28.3	18.6	58	19	23
334B	1.23	1.71	5.03	9.38	11.96	37.5	35.6	32.5	27.1	18.2	63	17	20
335A	1.09	2.17	10.66	12.95	14.18	33.1	31.3	29.5	26.1	22.4	62	19	19
335B	1.22	1.74	6.98	11.46	13.43	33.2	32.0	30.7	26.8	23.3	62	19	19
336	1.32	1.70	7.45	9.22	10.84	32.9	32.5	31.3	27.5	22.3	60	21	19
337	1.13	1.83	7.71	10.35	11.21	37.4	31.8	33.4	27.6	22.2	63	14	23
343	1.07	1.62	7.26	10.55	11.95	35.5	34.1	32.3	26.6	20.5	71	15	14
345	1.01	1.50	5.73	9.15	10.48	41.1	40.5	39.4	24.4	23.8	68	20	12
348	0.67	1.69	6.02	9.15	10.59	39.9	35.8	36.9	31.0	23.2	70	18	12
349A	1.18	2.55	7.15	10.33	11.70	0.0	35.9	30.1	24.4	20.2	66	20	14
349B	1.09	1.63	5.83	10.65	11.96	33.5	29.1	30.1	25.7	20.5	69	18	13
350A	1.99	3.00	7.93	10.23	11.45	35.7	33.7	31.0	25.8	20.8	66	21	13
350B	3.93	4.98	10.65	11.93	12.96	29.2	27.3	25.4	21.2	18.1	69	17	14

*Add 273.2 to convert to K.

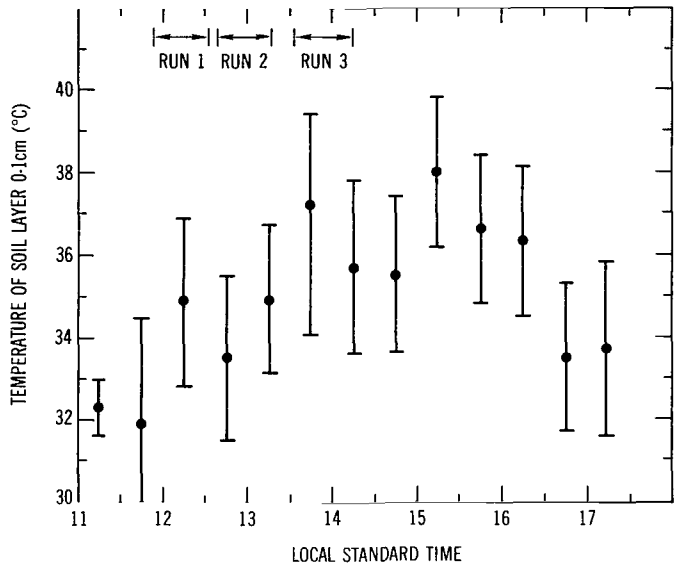

Figure 2. The average soil temperatures in °C (add 273.2 for K) of 0- to 1-cm from various fields as measured in half-hour intervals between 1100 and 1730 MST during the afternoon of April 5, 1974. The times of the three afternoon runs are marked for reference.

furrows relative to the flight lines are designated on the map (Appendix A) by the symbol ↔; the state of cultivation, listed or planted, is designated by L or P. No attempt has yet been made to estimate the power spectral density of the small-scale roughness features.

At the time of the predawn flight, soil samples were taken from six pairs of fields. The same sampling techniques as those described above were used with the exception that moisture samples were taken only from the top three layers. The restricted number of fields was dictated by the constraint that sampling be done at the time of flight and before sunrise effects perturbed the soil characteristics. The results of the predawn moisture measurements are given in the following section. A comparison of the moisture observed in the surface layer at dawn with that observed in the afternoon shows that the moisture did increase. A linear regression gives the relationship with a correlation coefficient of 0.964, where M_1.

$$M_1^{dawn} = 1.3 + 1.2\, M_1^{day} \tag{1}$$

is the moisture content of the surface layer. This increase of the moisture content is due to capillary flow from below and is normal for the soils of this area (Jackson, 1973). Condensation is unlikely since the dew point at the time of the predawn flight was 270 K (-3°C).

(a) Example of furrowed field

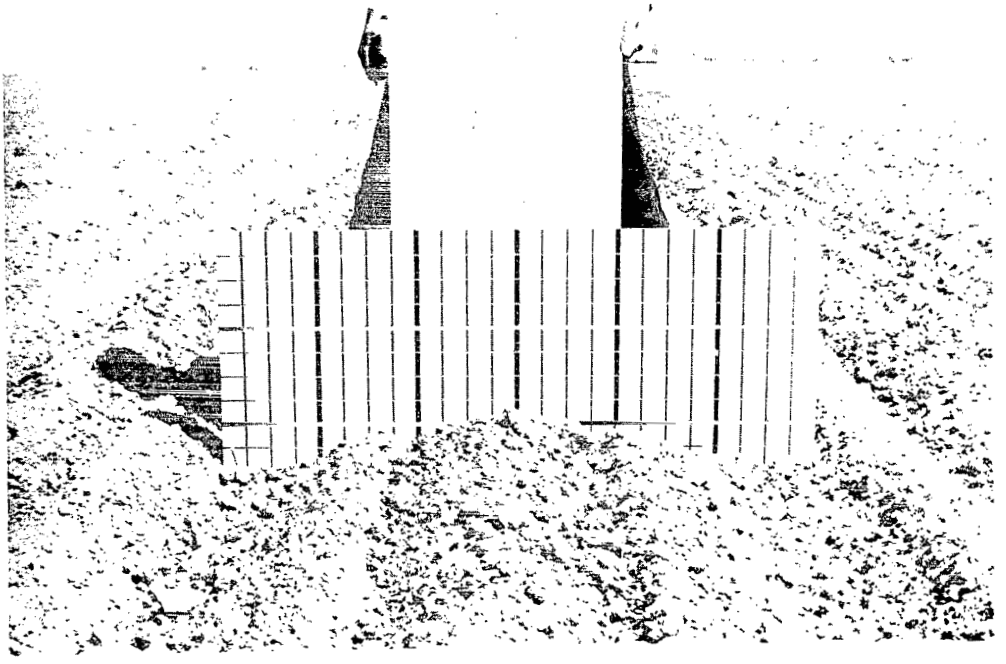

(b) Example of planted field

Figure 3. Photographs of two fields which were typical of the majority of fields sampled. The grid spacing is 5 cm. Although the bottom of the furrows were smoothed by irrigation, this was not true of all such fields.

RADIOMETRIC OBSERVATIONS

Surface Temperature Measurements

The data from the scanning infrared (IR) radiometer were recorded on film and were used to estimate the surface temperature of the individual fields. These data were calibrated using the results from the nonscanning radiometer which only recorded the surface temperatures of a narrow swath (2° beamwidth) directly below the aircraft; unfortunately the range of this radiometer was limited to temperatures below 313.5 K (40.5°C). The calibration procedure consisted of determining the relationship between film density and surface temperature for the range 298 to 313.5 K (25° to 40.5°C). These relationships were found to be linear with correlation coefficients greater than 0.98. This procedure was applied to the imagery obtained on each of the four (three afternoon and one predawn) passes over the four flight lines (Appendix A). The results for each field from the four passes are presented in table 3. It is expected that the accuracy is ±1 K in the temperature regions where the scanning and nonscanning radiometers overlap, at less than 313.5 K (40.5°C), while for temperatures above 313.5 K (40.5°C) the accuracy would be degraded to ±2 K at best. In particular, some of the values listed for run 3 appear unreasonably high (for example, greater than 323 K (50°C)) and should be disregarded.

From the viewpoint of developing algorithms for microwave remote sensing, it is necessary that we learn to correlate surface temperatures with the temperatures of the soil. The times at which the soil temperatures were measured in the various fields were noted by the investigators. It is thus possible to compare ground observations with nearly simultaneously observed aircraft observations. A linear regression was performed on the set of ground observations taken within 20 minutes of an overpass in comparison with infrared surface temperatures. We find that for both the afternoon and predawn data sets

$$T_{IR} = 1.34\, T_1 - 3.6$$

with a correlation coefficient of 0.96. T_{IR} is the observed surface temperature and T_1 the temperature measured in the first layer of soil.

21-cm Radiometer

The magnitude of the 21-cm brightness temperatures were determined by comparing the radiation received by the antenna with internal blackbodies at 381 K and 273 K. The calibration of the entire system was checked by flight lines over targets whose brightness temperatures could be calculated. These were over water and at an altitude of 6.1 km (20,000 ft) with the antenna looking at the cold sky (nadir angle of 159°). The results are listed below.

	Brightness Temperatures	
	Observed	Calculated
Over water	120.1 K	108 K
Sky	15.7 K	3.7 K

The calculated values included the effects of a dry atmosphere and used the water temperature of 288 K (15°C), observed by the infrared radiometer. The observed values are about 10 K higher than they should be at low brightness temperatures. This error would be expected to scale with the temperature difference from the internal blackbodies. Thus, for the range of values observed in this experiment, the error should be less than 5 K.

With a 15° beamwidth between half power points, the 21-cm radiometer averaged, over a considerable swath, a 200-m circle at nadir and 300- by 400-m area at a 40° nadir angle for an 800-m altitude. Because the down track field dimension was 400 m, the results obtained for the off nadir look-angle would include a certain amount of radiation coming from the adjacent fields. The results presented here are for the time when the beam spot was centered on the fields of interest. Table 4 is a listing of the results for the 21-cm wavelength radiometer; the results are presented for pairs of 400- by 400-m (40-acre) fields which were essentially identical in their surface characteristics. The soil moisture values are the averages at each depth for the eight sample points in each pair of fields. The observed range of brightness temperature is about 25 K for the nadir look-angles, with a similar range for the horizontal polarization at a 40° look-angle, and about one-half that for the vertical polarization. This small amount of variation is attributed to the relative dryness of the surface layer, that is, no field had a soil moisture value above 50 percent of field capacity in the 0- to 2-cm layer.

Table 5 is a listing of the 21-cm and infrared brightness temperatures for the early morning flight on April 6, 1974, along with the soil moisture values in the top three layers for those fields which were sampled that morning. The soil moisture values obtained the previous day are listed for comparison. Soil temperatures measured at the time of the predawn flight were between 281 and 283 K (8 and 10°C) for the 0- to 1-cm layer and between (15° and 18°C) for the 9- to 15-cm layer. The 21-cm brightness temperatures were generally 10 K lower for the early morning flight compared with a 25 to 30 K difference for the infrared surface temperatures. As a result, the 21-cm brightness temperatures listed in table 5 are approximately the same or greater than the infrared surface temperatures, which are listed for comparison. This is a consequence of the 21-cm radiometer sensing the higher subsurface temperatures noted above. Because the emitted radiation comes from a medium with a nonuniform temperature profile, the concept of a surface emissivity is misleading.

Table 3

Infrared Field Temperature Results from Flights on April 5 and 6, 1974, over Phoenix

Field Number	Infrared Temperature °C*			Morning Run	Field Number	Infrared Temperature °C			Morning Run
	Run 1	Run 2	Run 3			Run 1	Run 2	Run 3	
11	36.1	39.2	38.1	8.0	254	48.8	50.8	56.5	7.8
12	40.8	47.0	46.2	7.4	255	47.0	50.8	57.4	6.1
13	39.3	40.3	44.1	9.1	257	46.6	49.6	54.2	8.7
14	40.4	40.6	46.1	7.9	260A	33.1	33.6	35.6	9.2
38	40.8	47.0	44.7	6.6	260B	32.3	36.1	33.0	9.2
39	40.0	49.0	46.0	6.6	260C	35.6	38.5	38.6	9.2
42	42.9	50.6	48.3	6.5	260D	36.0	38.5	38.4	9.2
43	41.8	50.0	47.0	5.5	261A	38.1	48.0	41.8	9.3
51A	40.0	48.2	46.8	6.7	261B	35.9	38.3	37.4	8.9
51B	41.1	48.0	47.3	6.5	264A	46.6	48.2	52.5	9.8
60A	26.0	24.7	26.2	5.7	264B	44.6	46.9	48.1	9.8
60B	38.2	41.2	40.4	7.7	264C	48.0	47.4	53.9	10.1
61A	40.6	40.0	44.3	7.5	264D	46.2	47.1	50.0	9.6
62B	41.2	40.4	45.7	6.9	297A	41.2	41.2	44.6	9.5
99A	41.7	50.6	49.8	5.9	297B	42.7	44.3	44.9	9.4
99B	42.4	49.0	48.3	5.5	299	42.3	41.2	43.2	10.1
103A	40.0	45.1	47.3	5.9	300	40.3	41.7	42.9	9.9
104A	40.8	40.0	47.8	6.2	315A	41.6	42.2	46.9	9.5
104B	38.3	39.9	48.6	5.9	315B	45.0	48.3	52.8	8.5
105A	42.0	47.7	51.4	5.2	316A	43.3	46.6	51.1	9.5
105B	41.5	45.6	49.6	5.2	316B	45.2	49.0	54.1	8.6
106A	29.2	28.5	33.0	7.9	316C	43.2	46.4	51.8	9.7
106B	37.2	39.3	44.3	6.9	316D	45.4	49.8	54.1	9.1
106C	33.5	39.0	36.4	7.9	317A	36.0	39.4	37.9	9.8
107A	42.0	46.0	49.1	4.5	318A	42.7	43.2	50.0	9.5
107B	36.4	35.6	38.9	6.9	318B	42.0	44.3	49.0	9.1
121A	42.8	40.6	48.8	5.9	319A	26.3	27.4	28.8	7.8
121B	43.4	40.6	51.5	5.2	319B	26.4	27.2	29.0	7.9

*Add 273.2 to convert to K

Table 3 (Continued)

Field Number	Infrared Temperature °C*			Morning Run	Field Number	Infrared Temperature °C*			Morning Run
	Run 1	Run 2	Run 3			Run 1	Run 2	Run 3	
127	41.0	48.2	48.3	6.3	319C	32.0	33.9	35.7	8.0
131	42.2	47.5	47.5	5.6	319D	31.3	32.9	34.7	8.2
132	42.0	48.0	48.6	5.6	333A	37.8	40.4	40.0	9.4
237A	46.0	49.6	56.0	7.2	333B	46.6	49.8	52.3	8.8
237B	45.0	48.2	55.7	7.7	334A	47.4	48.8	53.6	9.2
242A	47.0	49.6	54.8	7.7	334B	47.4	49.4	54.5	9.6
242B	42.5	45.5	49.8	7.1	335A	43.2	47.1	47.7	9.2
243A	48.0	49.4	55.4	7.2	335B	43.5	46.9	47.7	11.2
243B	44.6	47.6	53.0	6.6	336	46.0	51.5	53.8	9.4
248A	45.2	42.9	49.3	7.7	337	44.4	48.3	48.8	8.8
248B	46.6	48.3	52.0	6.7	343	43.5	49.2	50.6	8.3
249A	45.0	44.3	50.3	6.7	345	44.1	48.8	51.6	8.3
249B	46.4	49.0	53.6	5.6	348	43.0	45.8	50.8	9.5
252A	47.4	47.7	51.8	6.3	349A	42.1	45.4	50.3	10.5
252B	46.2	49.6	53.3	6.1	349B	42.8	49.2	52.0	10.3
					350A	42.0	46.4	50.3	10.6
					350B	33.0	35.4	38.5	9.7

*Add 273.2 to convert to K.

Table 4
21-cm Brightness Temperatures Midday Results
for April 5, 1974, over Phoenix

Field Results		Nadir Results	40° Results		Percentage of Moisture by Weight					Texture		
			Horizontal Polarization (K)	Vertical Polarization (K)	0-1 cm	1-2 cm	2-5 cm	5-9 cm	9-15 cm	Sand	Silt	Clay
11	12	288.40	273.30	292.10	1.71	3.45	9.45	12.83	12.66	54	21	25
13	14	290.50	276.10	289.60	2.56	3.46	6.44	9.32	10.69	52	22	23
38	39	288.00	272.20	288.70	1.49	1.90	10.94	13.64	14.43	51	21	28
42	43	287.30	268.70	290.40	1.01	1.89	8.49	12.01	12.27	53	23	24
51	51	287.50	264.90	294.20	1.61	2.57	5.06	7.85	9.14	49	18	33
61	61	289.70	277.00	288.70	2.43	6.38	14.43	17.59	17.89	46	22	32
99	99	287.50	266.60	284.70	2.57	8.79	18.31	19.56	20.50	21	42	37
103	103	290.80	270.80	292.70	3.30	6.40	20.00	22.80	22.30	17	44	39
104	104	285.90	278.60	287.20	3.26	9.13	19.41	21.12	21.52	14	42	44
105	105	286.40	272.90	290.20	2.10	5.90	17.08	19.95	21.08	17	41	42
106	106	270.70	273.90	285.20	6.70	12.80	22.20	25.70	26.70	17	41	42
107	107	290.20	275.30	293.00	4.20	7.60	15.00	21.50	23.30	19	38	43
121	121	290.30	283.80	290.20	1.34	3.52	10.30	14.16	18.27	46	30	24
127	127	289.60	278.70	295.10	1.03	2.03	6.91	11.70	14.61	41	25	34
131	132	287.90	277.60	293.40	1.33	2.49	8.18	14.31	16.24	43	25	32
237	237	292.90	274.70	293.90	1.31	3.03	9.44	13.21	15.15	39	22	39
242	242	292.30	277.90	297.40	1.64	3.32	7.79	11.57	13.83	44	20	36
248	248	286.60	275.80	288.40	5.16	7.68	12.01	17.18	19.79	32	20	48
249	249	293.20	281.80	289.60	1.83	4.72	13.63	19.96	20.03	24	24	52
252	252	294.90	283.10	293.50	1.45	3.22	10.12	15.19	17.36	35	25	40
255	255	288.00	269.60	283.20	2.96	6.63	15.50	19.38	20.48	34	16	50
260	260	274.90	262.60	279.20	9.24	13.92	18.84	20.02	21.05	39	16	45
261	261	287.10	273.00	290.20	3.00	10.40	17.40	19.40	19.90	42	17	41
264A	264	291.10	283.60	291.30	2.09	4.35	12.12	14.90	16.31	48	14	38
264C	264	288.40	282.60	291.70	2.06	4.14	10.87	13.84	14.68	58	13	29
297	297	289.30	272.00	288.20	2.36	4.61	10.63	14.18	15.42	57	14	29

Table 4 (Continued)

Percentage of Moisture by Weight												
Field Results		Nadir Results	40° Results		0-1 cm	1-2 cm	2-5 cm	5-9 cm	9-15 cm	Texture		
			Horizontal Polarization (K)	Vertical Polarization (K)						Sand	Silt	Clay
299	300	284.80	267.20	287.70	2.84	6.55	13.59	15.72	16.72	59	9	32
315	315	296.70	282.50	292.40	1.55	5.03	12.32	14.41	15.25	53	16	31
316A	316	293.50	282.50	293.00	1.70	4.40	14.20	16.00	17.00	50	19	31
316C	316	295.30	280.20	293.10	1.30	1.90	8.60	12.80	15.00	63	15	22
317	317	281.00	261.00	288.50	2.00	3.20	6.50	10.50	13.20	52	17	31
333	333	287.20	279.00	286.30	1.40	2.00	5.30	9.60	10.30	66	18	16
334	334	287.40	275.80	287.20	1.27	1.70	5.92	9.84	11.50	61	18	21
335	335	293.50	281.80	290.60	1.03	1.79	7.59	10.69	12.11	62	19	19
336	337	291.50	280.60	290.00	1.20	1.80	7.60	9.50	11.00	61	18	21
345	348	291.90	274.80	291.40	0.71	1.41	5.14	7.89	9.21	69	19	12
349	349	297.20	277.50	290.80	1.10	2.10	6.50	10.50	11.80	68	19	13
60A	60B	254.40	233.00	265.20	15.10	17.30	20.87	22.06	22.40	50	21	29

Table 5
21-cm Brightness Temperatures Predawn Results
for April 6, 1974, over Phoenix

Field Pairs		Brightness Temperatures		Soil Moisture in Weight Percent							
				Same Day (cm)			Previous Day (cm)				
		L-Band (21 cm) (K)	IR	0-1	1-2	2-5	0-1	1-2	2-5	5-9	9-15
11	12	279.4	7.4				1.7	3.5	9.5	12.8	12.7
38	39	277.9	6.7				1.5	1.9	10.9	13.6	14.4
42	43	276.4	6.1				1.0	1.9	8.5	12.0	12.3
51	51	277.9	6.6				1.6	2.6	5.1	7.9	9.1
60	60	237.1	8.0								
99	99	276.1	4.8				2.6	8.8	18.3	19.6	20.5
105	105	277.0	5.5	5.6	9.9	16.2	2.1	5.9	17.1	20.0	21.1
107	107	277.8	5.4				4.2	7.6	15.0	21.5	23.3
127	128	280.6	6.3				1.0	2.0	6.9	11.7	14.6
131	132	281.3	6.4				1.3	2.5	8.2	14.3	16.2
237	237	282.1	6.7	3.4	4.5	10.4	1.3	3.0	9.4	13.2	15.2
242	242	279.5	6.6				1.6	3.3	7.8	11.6	13.8
243	243	282.2	7.4				2.0	3.6	7.1	12.7	15.5
248	248	278.0	5.0				5.2	7.7	12.0	17.2	17.8
249	249	284.0	7.0				1.8	4.7	13.6	20.0	20.0
252	252	282.5	6.3				1.5	3.2	10.1	15.2	17.4
255	257	277.7	8.9				3.0	6.6	15.5	19.4	20.5
260	260	267.1	8.2	12.4	15.6	20.7	9.2	13.9	18.8	20.0	21.0
261	261	275.3	8.7				4.1	10.6	17.9	19.5	20.3
264A	264	284.0	9.9				2.1	4.4	12.1	14.9	16.3
264C	264	283.6	10.5				2.1	4.1	10.9	13.8	14.7
297	297	277.5	8.8				2.4	4.6	10.6	14.2	15.4
299	300	280.8	9.5	4.4	5.6	12.3	2.8	6.6	13.6	15.7	16.7
315	315	283.2	9.0				1.6	5.0	12.3	14.4	15.3
316A	316	281.6	9.6	2.8	4.7	12.5	1.7	4.4	14.2	16.0	17.0

Table 5 (Continued)

Field Pairs		Brightness Temperatures		Soil Moisture in Weight Percent							
				Same Day (cm)			Previous Day (cm)				
		L-Band (21 cm) (K)	IR	0-1	1-2	2-5	0-1	1-2	2-5	5-9	9-15
316C	316	281.9	9.6				1.3	1.9	8.6	12.8	15.0
							3.7	5.4	10.8	13.6	14.8
317A	317	267.8	10.0				2.1	3.2	6.5	10.5	13.3
317C	317	269.1	9.9								
							4.4	7.5	11.5	13.4	14.2
333	333	265.9	8.6								
334	334	277.1	10.0				1.3	1.7	5.9	9.8	11.5
335	335	280.1	9.1	1.7	2.5	8.2	1.0	1.8	7.6	10.7	12.1
337	336	281.9	8.6				1.1	1.8	7.7	10.4	11.2
345	348	279.6	8.7				0.7	1.4	5.1	7.9	9.2
349	349	281.6	9.7								
							2.8	3.7	8.5	9.8	10.8

2.8-cm Radiometer

The 2.8-cm scanning radiometer consists of three basic components: a phased array antenna, a beam steering computer, and the microwave receivers for the horizontal and vertical channels. The antenna is a dual polarized, electrically scanned, phased array which consists of 51 linear slotted waveguide sections forming a 109- by 91-cm aperture. The microwave receivers operate at a center frequency of 10.69 GHz with a 150-MHz bandwidth. The magnitudes of the resulting brightness temperatures are determined by comparison with internal blackbodies at 323 K and 403 K. The algorithms for computing the brightness temperatures for this system are currently undergoing revision. The resulting modifications in these algorithms should produce only a uniform shift in brightness temperature and not affect the conclusions presented here.

The data for the 2.8-cm scanning radiometer were recorded at 44 beam positions for each scan. The scan rate was adjusted to provide contiguous coverage, which for the altitude and velocity of these flights was one scan per second. The brightness temperatures for each beam position were printed in a map-like format on which the individual fields could be located. The locations of the beam positions on the map were partially corrected for aircraft pitch and roll by the computer mapping program. However, there were some errors in the geometric algorithms incorporated in the original processing of the data which have not been corrected. Therefore, minor errors in the locations of beam positions near the field boundaries occurred. When such errors were apparent to the investigators, the errant beam positions were deleted from the group used to determine the average brightness temperature for the affected field. As will be noted later, the results indicate that all such errors were not located and deleted.

For the 400- by 400-m (40-acre) fields and an altitude of 800 m, there were between 50 and 100 data points; the average brightness temperature and standard deviation were calculated for each. The standard deviations were less than 5 K for dry fields and between 5 and 10 K for wet fields, which is indicative of the greater variability of moisture in the wet fields. These average brightness temperatures were determined for approximately 90 fields on each on the four passes over the fields. The results for both polarizations are presented in table 6. The results are presented graphically in figures 4a and 4b for the two polarizations for the midafternoon flight. The correlation coefficients for these two cases were in the 0.75 to 0.80 range. The slope for the horizontal polarization is 0.34 K/percent of field capacity (FC), which for heavy soils (high percentage clay, FC = 30 percent) translates to 1.1 K/percent soil moisture and for light soils (low percentage clay, FC = 20 percent) translates to 1.7 K/percent soil moisture. For the vertical polarization, the slopes were 20 percent less. The slopes for the predawn runs were also decreased by a similar amount which indicated that there was a greater difference between the wet and dry fields for the midafternoon runs than for the predawn run.

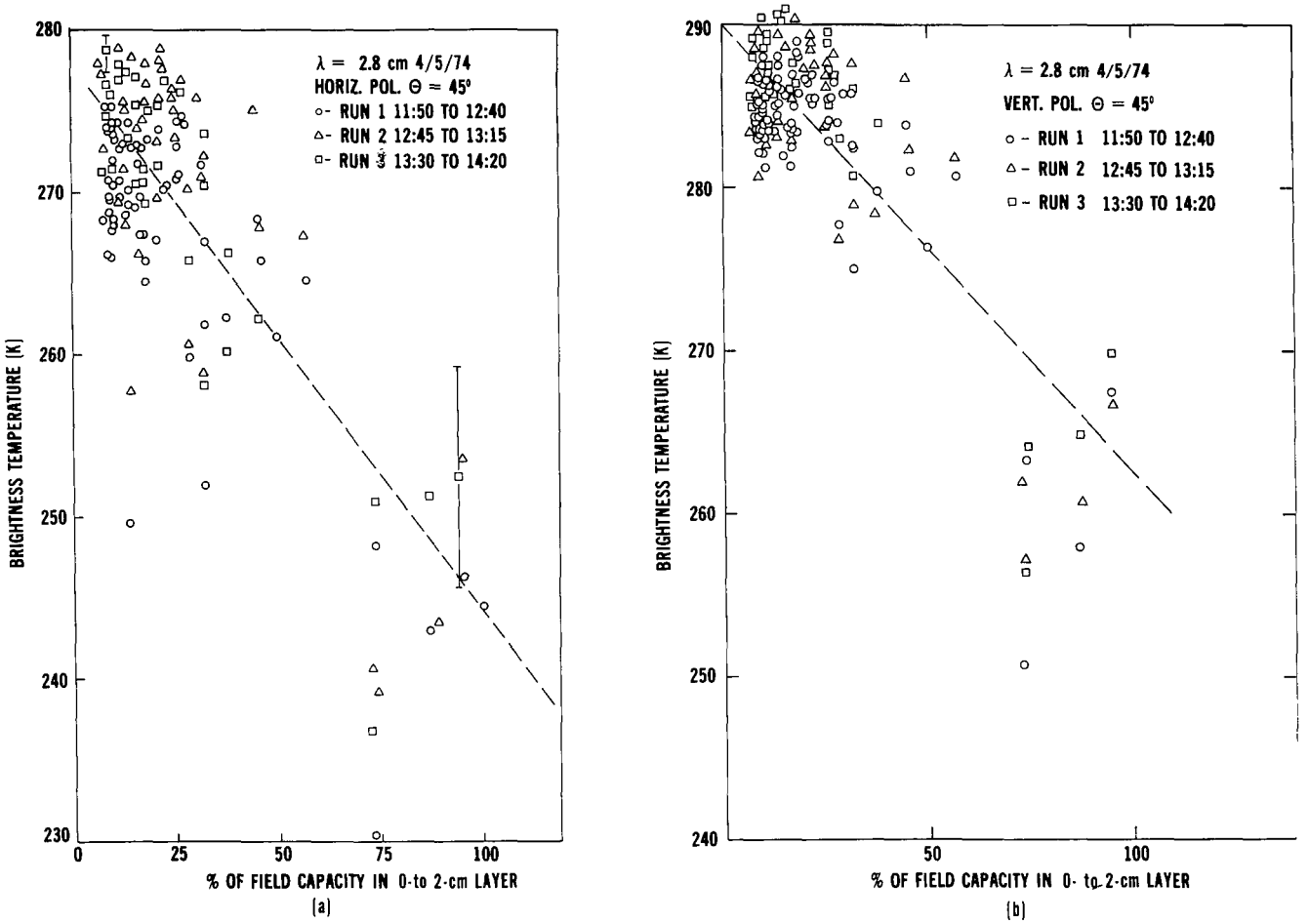

Figure 4. Brightness temperatures for 2.8 cm plotted as a function of soil moisture in the 0- to 2-cm layer expressed as the percent of field capacity for the soil. The dashed lines are linear regression fits to the data. (a) Horizontal polarization; the error bars indicate the standard deviations for a wet and dry fields. (b) Vertical polarization.

Table 6
2.8-cm Brightness Temperatures (K)
April 5 and 6, 1974, over Phoenix

Field Number	Horizontal				Vertical			
	Run 1	Run 2	Run 3	Run 4	Run 1	Run 2	Run 3	Run 4
11	267.5	274.0	270.6	244.8	281.3	286.0	286.0	258.0
12	269.1	275.5	271.8	240.4	282.0	285.5	286.3	259.1
13	275.0	273.2	276.2	245.6	287.0	285.5	287.5	260.5
14	274.5	269.4	274.5	243.3	284.9	284.2	286.0	261.9
38	267.6	270.8	271.5	243.1	285.1	286.3	288.3	259.8
39	266.0	271.8	271.0	242.0	284.4	285.8	288.4	259.4
42	268.1	269.1	270.4	241.2	286.4	287.0	290.5	261.0
43	266.2	269.9	268.0	239.7	285.1	286.6	289.1	261.1
51A	273.2	276.9	275.4	242.7	283.9	286.8	288.5	257.1
51B	273.5	277.2	275.8	241.4	284.8	286.8	289.3	256.6
60A	229.6	240.4	236.9	215.8	250.7	262.0	256.4	235.0
60B	260.1	260.8	267.5	206.9	281.3	273.7	285.6	228.6
61A	****	271.8	270.6	246.5	****	285.3	285.9	260.1
62B	273.9	273.1	275.5	245.7	286.5	287.8	288.4	260.9
99A	273.4	277.0	275.2	246.1	285.8	288.2	290.3	258.2
99B	274.3	276.0	275.9	245.8	285.5	287.8	289.5	258.2
103A	269.6	271.5	274.4	243.7	284.5	283.4	287.9	257.2
104A	270.1	275.1	273.4	244.2	283.4	286.4	286.5	255.8
104B	270.9	275.4	275.9	243.2	283.9	286.8	287.3	257.1
105A	270.1	275.1	274.7	243.5	286.7	286.8	290.7	257.6
105B	272.7	274.1	275.0	242.6	286.1	285.8	290.3	257.6
106A	246.3	253.5	252.5	231.3	267.5	266.7	269.8	245.6
106B	267.0	272.2	273.7	243.0	282.5	285.5	286.0	258.5
106C	261.9	271.0	270.4	241.7	282.6	286.3	235.9	257.2
107A	272.9	278.3	277.2	243.6	285.7	288.6	290.9	255.9
107B	271.0	276.3	276.1	242.2	282.9	286.4	288.8	255.5
121A	270.8	273.1	274.8	247.6	283.0	295.1	285.2	262.6
121B	271.7	272.6	275.4	245.8	283.7	285.8	285.7	261.5

Table 6 (Continued)

Field Number	Horizontal				Vertical			
	Run 1	Run 2	Run 3	Run 4	Run 1	Run 2	Run 3	Run 4
127	273.8	278.7	275.8	247.6	283.5	289.6	287.8	261.7
131	273.9	277.2	278.8	249.5	284.1	288.6	289.0	262.2
132	274.3	278.1	277.9	250.4	284.1	289.2	288.9	262.5
237A	273.1	271.3	****	246.4	287.5	289.2	****	260.4
237B	271.5	271.4	****	246.3	286.7	288.7	****	260.4
242A	273.7	275.3	****	248.0	288.1	289.3	****	259.0
242B	273.7	274.3	****	245.6	286.4	288.2	****	257.3
243A	271.2	274.6	****	245.9	286.9	287.8	****	257.0
243B	271.6	274.8	****	243.5	286.6	288.0	****	257.3
248A	272.9	274.3	274.2	243.9	284.1	285.0	285.0	258.6
248B	270.5	277.7	276.9	243.7	285.6	288.5	289.1	259.2
249A	273.0	275.7	275.4	241.7	285.0	284.4	286.1	258.2
249B	272.6	277.5	277.1	242.4	286.3	286.7	287.5	258.9
252A	273.8	278.0	276.4	243.0	287.5	287.2	289.3	261.5
252B	274.3	277.7	276.7	242.8	288.0	285.9	289.5	261.7
254	272.0	275.6	****	246.7	288.1	290.5	****	259.8
255	271.5	276.8	****	248.7	288.3	291.9	****	262.1
257	271.5	277.9	****	247.9	289.1	292.1	****	262.3
260A	265.9	267.7	****	238.7	281.1	282.2	****	251.6
260B	264.6	267.4	****	236.6	281.8	281.7	****	251.7
260C	271.7	275.6	****	244.0	285.8	287.6	****	255.7
260D	268.3	274.9	****	240.7	283.9	286.8	****	254.3
261A	274.2	277.1	****	244.7	286.5	288.4	****	257.4
261B	270.2	275.9	****	242.5	285.2	287.3	****	256.7
264A	274.6	278.9	****	249.4	287.0	289.3	****	261.1
264B	272.6	278.9	****	246.9	286.1	288.6	****	259.6
264C	272.8	278.2	****	249.5	285.6	290.0	****	261.9
264D	269.6	278.0	****	247.5	287.5	288.5	****	261.6
297A	265.8	270.2	270.5	236.2	285.0	285.8	286.8	259.5
297B	267.1	269.7	271.7	236.2	286.7	267.2	287.5	258.6

Table 6 (Continued)

Field Number	Horizontal				Vertical			
	Run 1	Run 2	Run 3	Run 4	Run 1	Run 2	Run 3	Run 4
299	265.3	270.6	****	240.4	285.8	285.9	****	258.1
300	264.9	270.1	****	238.0	284.1	285.8	****	257.3
315A	274.2	274.8	277.4	246.8	286.2	283.9	287.6	258.6
315B	274.8	274.6	276.2	247.4	285.6	284.1	276.2	259.2
316A	272.7	271.3	275.0	247.7	283.4	282.7	286.4	259.9
316B	270.7	271.0	273.3	245.9	283.9	283.0	287.0	261.2
316C	271.2	270.4	273.4	245.5	284.4	285.6	285.6	259.7
316D	270.5	271.1	271.7	245.5	284.6	280.8	286.7	260.8
317A	249.5	257.8	****	231.2	285.0	286.6	****	261.0
318A	268.2	270.5	271.3	240.7	285.0	283.8	287.9	258.6
318B	269.1	268.1	272.9	243.6	284.5	283.4	287.3	256.7
319A	243.0	242.9	251.5	220.4	258.0	260.7	264.8	242.6
319B	248.2	239.1	251.0	224.6	263.4	257.0	264.1	241.5
319C	259.8	250.6	265.9	232.2	277.8	276.8	283.1	253.0
319D	262.3	260.2	266.4	235.3	279.8	278.5	283.9	263.6
333A	267.4	266.2	271.5	243.5	282.5	282.7	286.7	258.7
333B	268.2	269.3	272.9	246.9	283.6	283.8	286.4	258.7
334A	272.6	272.8	****	247.7	283.0	284.0	****	258.6
334B	272.4	273.7	****	246.2	283.4	285.5	****	260.2
335A	272.0	271.8	273.7	247.9	282.1	282.8	284.8	259.4
335B	269.7	272.9	271.9	250.4	282.2	282.8	284.6	260.2
336	275.3	275.2	276.6	240.8	284.4	284.9	287.9	260.7
337	275.3	274.1	276.8	250.9	283.3	283.1	286.2	261.6
343	273.5	274.3	274.8	249.1	283.6	283.8	287.2	260.1
345	269.6	273.7	273.3	247.6	283.3	286.5	288.4	262.0
348	268.7	272.4	272.7	246.9	285.3	287.1	289.3	263.2
349A	268.5	272.7	269.9	245.6	283.5	285.5	285.7	262.4
349B	268.3	273.4	271.6	244.7	285.1	286.9	288.5	263.4
350A	264.5	272.2	269.4	243.3	283.6	285.2	287.7	262.7
350B	252.1	258.9	258.2	235.0	275.1	279.0	280.7	259.2

DISCUSSION

Recently, Burke and Paris (1975) developed a radiative transfer model for the emission of microwave radiation from bare agricultural soils. Their results suggest that instead of considering T_v and T_H individually, they should be considered in the combinations: $P = \frac{1}{2}(T_v + T_H)$ and $Q = T_v - T_H$. These quantities are recognized as the first two Stokes parameters. The model has been used to calculate P and Q using soil and moisture profiles similar to those found at the time of the April 5 flight. The dielectric coefficients used in the calculations were those determined at the Texas A&M Laboratory (Babai, 1974; Newton and McClellan, 1975) with Phoenix soils in X- and L-band waveguides. Somewhat surprisingly, the model shows great sensitivity to the near surface moisture but little response to the moisture gradient. The reasons for this result differ for X- and L-bands. Although the radiation reaching the antenna comes from near the surface for the X-band and from deep down for the L-band, the total radiation emitted (and thus observed by an antenna) only weakly depends on whether the moisture gradient near the surface is gentle or sharp. Calculations by Schmugge et al. (1974) using a similar radiative transfer model* have indicated that the emission from the surface of a soil is determined by the dielectric properties of a layer a few tenths of a wavelength thick. Based on these results, Cihlar and Ulaby (1975) suggested that this effect is due to the dominance of the Fresnel coefficient at the airsoil interface over all intersoil processes. The results of the calculations shown in figures 5a and 5b have X-band values of P and Q, respectively, plotted as a function of soil moisture in weight percent for the top layer. The different curves represent values at various look-angles (θ_0). The $\theta_0 = 0°$ and $\theta_0 = 30°$ curves in figure 5a are indistinguishable. The $\theta_0 = 50°$ curve, at most, varies by 3 K from the $\theta_0 = 30°$ curve over the moisture range 1 to 25 percent. Thus, the model predicts that P is almost independent of look-angle in the range $0° \leqslant \theta_0 \leqslant 50°$. Although the magnitudes of Q shown in figure 5b differ with look angle, they show similar moisture dependences. Q increases with M_1 in the range $0 < M_1 < 12$ percent, then remains near constant for $M_1 > 12$ percent. If for simplicity we were to assume that the primary effect of surface roughness is to change the effective look direction of the antenna (which is true in the geometric optics limit), then Q would be considered sensitive to surface roughness but not P. By changing the average temperature profile to that of the morning flight we find that P is sensitive to temperature variations but Q is not. For example, a shift of 20 K in the temperature of the surface layer changes Q in the direction of the shift by < 2 K, while P is changed by ~ 15 K. Similar results are predicted for the L-band radiation.

The purpose of this section is to consider the radiometer data in terms of P and Q. The Burke-Paris model is used as a qualitative guide to alert us as to which way physical parameters should shift under various soil moisture-temperature situations. At times, the data

*Wilheit, T. T., "Radiative Transfer in a Plane Stratified Dielectric," private communication, March 1975.

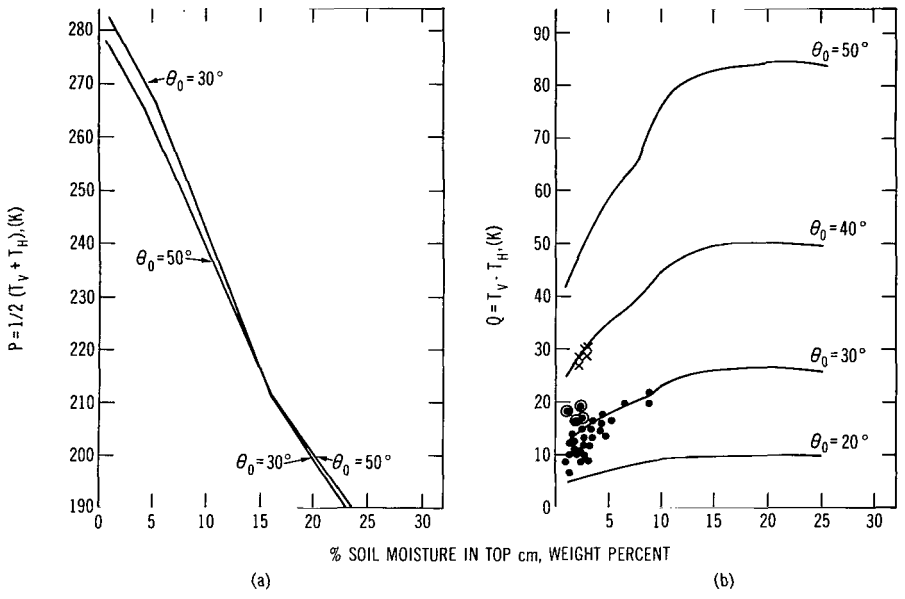

Figure 5. Predictions of P(a) and Q(b) by a radiative transfer model for 2.8-cm emissions at various look angles θ_0. Values of Q observed for the afternoon run are plotted in (b) X—flat fields, ○—planted fields, and ●—furrowed fields.

are compared with the moisture found in the i^{th} layer M_i or the average moisture down to the i^{th} layer $\langle M_i \rangle$, and at other times to the percent of field capacity F_i or $\langle F_i \rangle$. Here F_i is defined as the percent moisture observed in the i^{th} layer divided by field capacity (FC) and multiplied by 100. This quantity is introduced to eliminate soil texture as a parameter and is discussed in Appendix B.

During the predawn flight, the air was relatively still in comparison with the air during the afternoon flight. Atmospheric turbulence introduced some aircraft drifts and rolls during acquisition of afternoon data. These motions had the effect of introducing a degree of confusion in determining which data belong to adjacent fields. A comparison of the data set (table 6) with microwave imagery shows that our failures are signaled by a shift of several degrees in the value of Q from one daytime run to the next. The data set was examined to find the runs for which the value of Q is most representative of the fields (that is, have no smearing from adjacent fields). This procedure is justified because the value of Q is largely insensitive to the shifts in soil temperature observed during the afternoon [figure 2]. The values of Q as a function of M_1 are superimposed on figure 4b as a scatter plot. We note that all but a few points fall between the $\theta_0 = 30°$ and $\theta_0 = 20°$ curves. The major exceptions are fields 317 (marked by the symbol X) and fields 28, 29, 42, and 43 (symbol 0). Recall that field 317 was flat. Fields 38, 39, 42, and 43 were all planted and relatively smooth. The effects of small scale roughness is to move the value a smaller amount from specular values than the larger scale roughness. In general, the effects of roughness are more pronounced in listed than in planted fields. Considering only the fields with $F_1 < 10$, we find that for listed fields $\langle Q \rangle = 12.2 \pm 2.0$ K, while for planted fields, $\langle Q \rangle = 14.2 \pm 2.6$ K.

Had the fields been perfectly smooth, we would expect values of Q between 40 K and 50 K at this moisture range. We note that for $M_1 \leq 15$, the value of Q unambiguously increases with moisture. However, on the basis of Q values alone, it is not possible to distinguish a wet rough field from a smooth dry one because both would have values of ~30 K. Figure 5a suggests that they should have quite different P values.

An interesting feature related to sun angle was observed in the 21-cm data and restricts our ability to derive moisture information from observed Q values. Flight line 1 was flown south-to-north observing T_H and north-to-south observing T_v. Thus, the antenna viewed the hot side of clods and furrows while measuring T_H and the cold side while measuring T_v. Line 2 was flown in the reverse sequence. We expect then to find the values of Q compressed along line 1 and enhanced along line 2. In measuring P along these lines the effects should be offsetting. Because the flights were performed in the early afternoon, the effect was of smaller magnitudes along the east-west lines. The average values of P and Q observed along the four lines are:

Line	P (K)	Q (K)
1	283.8 ± 2.3	9.9 ± 2.3
2	278.4 ± 9.9	19.6 ± 4.4
3	283.8 ± 3.5	11.2 ± 4.7
4	281.2 ± 5.6	16.7 ± 5.2

If the very wet field No. 60 is not considered in the data, the value of P along line 2 becomes 281.3 ± 4.0 K, and Q becomes 18.4 ± 2.1 K. These results indicate that unless both polarizations can be observed simultaneously, sun angle effects can be quite important.

Figure 6 is a plot of the values of P observed along the first run as a function of F_1 for both 2.8-cm and 21-cm observations. Where possible, we have combined pairs of fields in presenting X-band data and made use of the fact that the nadir view combines the polarizations to give us P at $\theta_0 = 0°$. A linear regression study of the data sets shows that for X and L bands:

$$P_X = 287.1 - 1.05\, F_1 \tag{2}$$

and

$$P_L = 300.7 - 1.23\, F_1 \tag{3}$$

with correlation coefficients of -0.88 and -0.89, respectively. A similar regression performed on the 21-cm data with P_L as a function of the average percent field capacity of the 0- to 2-cm layer gives

$$P_L = 297.0 - 0.53 \langle F_2 \rangle \tag{4}$$

with a correlation coefficient of -0.73, where $\langle F \rangle$ is the percent of field capacity in this layer. A comparison of observed values of P_X and P_L for the pairs of fields yield the linear

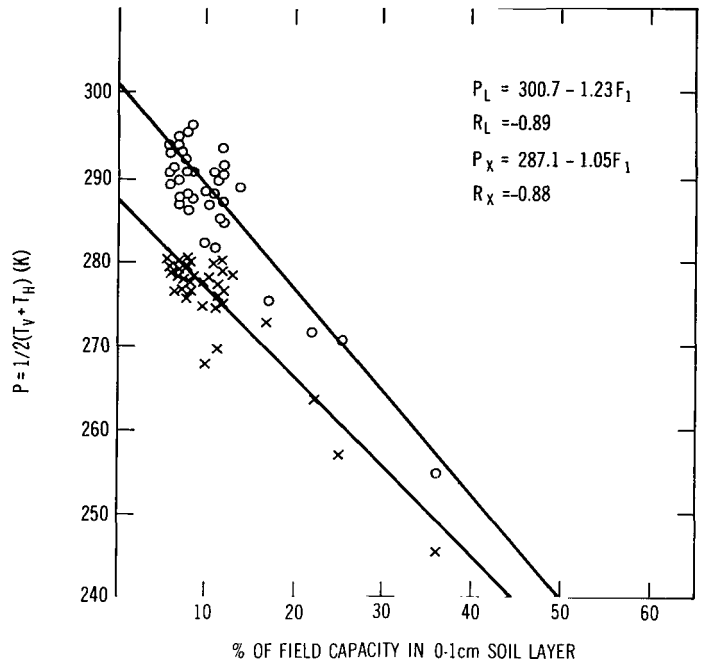

Figure 6. Plot of observed 21-cm (○) and 2.8-cm (X) values of P for pairs of fields from run 1 of the afternoon flight as a function of the percent field capacity in the 0- to 1-cm layer.

regression

$$P_L = 1.04\,P_X + 0.64 \tag{5}$$

with a correlation of 0.903. The decrease in the correlation coefficient with depth combined with the relatively high correlation between P_L and P_X tends to confirm the hypothesis that surface effects dominate over those of the subsurface region.

The morning ground truth set, with which we compare the microwave data (table 5), is limited to six fields. Linear regression analyses of X- and L-band intensities as a function of the percent field capacities of the 0- to 1-cm layer (F_1) give

$$P_X = 256.4 - 0.27F_1 \tag{6}$$

$$P_L = 286.4 - 0.40F_1 \tag{7}$$

with correlation coefficients of –0.94 and –0.93, respectively. A comparison of these relationships with equations 2 and 3 shows that the X-band brightness temperatures are changed more dramatically in magnitude than the L-band results. The reason for this effect lies in the fact that the major contributions to the L-band total intensity lie deeper in the soil than those of the X-band. Because the temperatures of deeper layers vary less than those of the surface layers, the result is not surprising. A second point of difference is the change of

slopes. This is a moisture-temperature effect. Due to the relatively high heat capacity of water, the physical temperatures of moist soils respond less quickly to changes of air temperature than dry soils. Consider the surface temperatures of fields 335 and 260. During the first afternoon run, the surface temperatures were 316 K and 306 K (43° C and 33° C), respectively. At the time of the dawn flight they were 283.2 K and 282.2 K (10.2° C and 9.2° C). Because of the correlation between the surface temperature and that of the top layers of the soil, the overall effect is to produce a rotation of the curve toward a lower slope as we pass from afternoon to dawn observations.

A linear regression was also performed on the 2.8- and 21-cm data for those pairs of fields which were available from the dawn flight. The relationship is given by

$$P_L = 1.32\, P_X - 54.9 \qquad (8)$$

with a correlation coefficient of 0.893. The increased slope in comparison with the afternoon value (equation 5) results from the soil temperature effects noted in the previous paragraph.

Information concerning the relative moisture status of the top layer of soil can be deduced from a comparison of afternoon and dawn microwave data sets. We have seen that Q is dependent on soil moisture and look-angle as mediated by surface roughness. By comparing microwave observations from the same fields on the afternoon run, run 1, with those at dawn, we hold the roughness (effective look-angle) constant. The Burke-Paris model predicts that if the moisture is held constant and the temperature decreases by 20 K, the value of Q should decrease by ~ 2 K. If, on the other hand, the moisture increases, the value of Q should also increase. Figure 7 is a scatter plot of observed morning values of Q as a function of the afternoon observed values. The line $Q_{dawn} = Q_{day} - 2$ is drawn for reference. We find that all but 6 fields out of 96 fall on or above this line. One of the fields, 60A was very wet during the day. We expect that it should be less moist during the dawn flight due to evaporation from the surface and percolation into the soil. The other fields were all from line 4 which was observed last. They probably are representative of a sunrise effect on the surface. We believe that this general shift in the observed values of Q constitutes the microwave signature of the surface rewetting phenomena described by Jackson (1973).

SUMMARY AND CONCLUSIONS

The primary goal of the April 5 and 6, 1974 flights over the Phoenix site was to study the feasibility of quantifying the effects of the nonuniform vertical distribution of moisture, surface roughness, and soil type. Despite the disappointing range of moisture in the surface layers of the studied fields, the mission was productive. Our understanding of the microwave signatures of agricultural scenes and how these signatures can be exploited to give us the information we seek has been enhanced considerably. Some of new items of understanding include:

- By simultaneously observing T_v and T_H we can form the parameters $P = \frac{1}{2}[T_v + T_H]$ and $Q = T_v - T_H$. It has been shown that moisture and surface roughness effects can be separated by a comparison of these parameters.

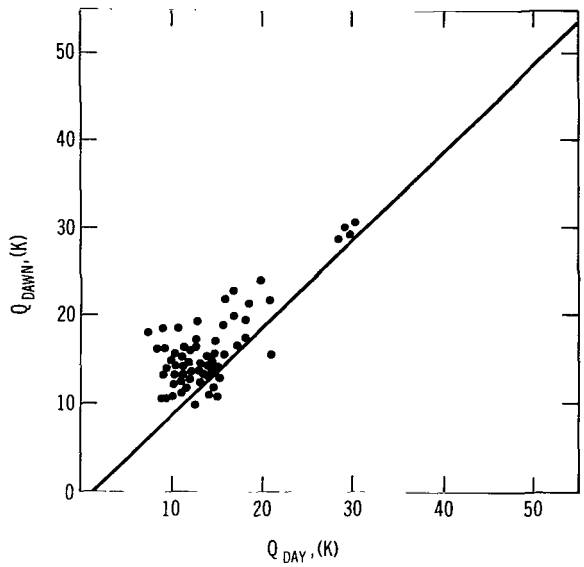

Figure 7. Scatter plot of observed 2.8-cm values of Q taken at dawn as a function of their values during the previous afternoon.

- By comparing afternoon and dawn observations of P for the X- and L-bands, we found that the P versus F slope depends on the time that the observation is made, with the afternoon observations yielding the greater slope. The improved correlation obtained when soil moisture is expressed as a percent of field capacity (F) indicates that the effects of soil type can be quantified.
- By comparing the values of Q as observed during the afternoon and dawn flights, we find that the microwave signature of the surface rewetting effect described by Jackson (1973) is an increase in the polarization. As yet, the data set is too small to calibrate the change of Q with the amount of water has moved to the surface.
- By comparing the response of P_X and P_L to the changes between afternoon and dawn, we confirmed the prediction of a radiative transfer theory that the 21-cm radiation reaching the antenna comes from much deeper in the soil than the 2.8-cm radiation. However, the high correlation (~0.9) between P_X and P_L observed in both the afternoon and predawn data confirms the somewhat paradoxical hypothesis that the surface layer dominates over subsurface gradient effects at both wavelengths.

This final conclusion is a major disappointment. It was hoped that gradient information could be obtained by comparing 2.8- and 21-cm observations. Perhaps a study based on a wider variety of moisture profiles will suggest a way around the impass.

Results have indicated that the effect of soil type is well understood and that emission from the soil is dominated by the dielectric properties of the surface layer, which for this case was 1 or 2 cm thick. In addition, these results have indicated a possible new approach, that is, the use of Stokes parameters, in our efforts to quantify the effects of surface roughness. To verify the usefulness of these parameters for separating the effects of roughness and soil moisture, data over a wider range of moisture conditions is required. To accomplish this, the experiment was essentially repeated in March 1975 with several significant changes. By moving the flight to mid-March, we increased the probability of observing the needed wider variety of moistures. The altitude of the off nadir runs was decreased to reduce the footprint of the 21-cm radiometer. Additional nonscanning radiometers were added with wavelengths of 1.67, 1.36, and 0.8 cm. The data from this experiment are still being reduced for analysis.

ACKNOWLEDGMENTS

The authors would like to express their appreciation to Drs. H. Bouwer, R. Jackson, and R. Reginato of the U. S. Water Conservation Laboratory at Phoenix for allowing us to use their facility as a base of operation for this experiment. Their help and advice made the large scale ground truth acquisition in this experiment possible.

Goddard Space Flight Center
National Aeronautics and Space Administration
Greenbelt, Maryland March 31, 1976

REFERENCES

Babai, P., "Measurement of the Complex Dielectric Constant of Soils at X-Band," Technical Memorandum No. 95, Remote Sensing Center, Texas A&M University, June 1974.

Basharinov, A.E., L.F. Borodin, and A.M. Shutko, "Passive Microwave Sensing of Moist Soils," *Proc. of URSI meeting on Microwave Scattering and Emission from the Earth*, Berne, Switzerland, September 1974, pp. 131-136.

Burke, W. J. and J. F. Paris, "A Radiative Transfer Model for Microwave Emissions from Bare Agricultural Soils," JSC-09836, NASA TM X-58166, 1975.

Burke, W.J. and J.F. Paris, "Remote Detection of Soil Moisture by the Passive Microwave Imaging System," *Trans. American Geophys. Union*, **56**, 1975, p. 359.

Cihlar, J. and F.T. Ulaby, "Microwave Remote Sensing of Soil Water Content," RSL Technical Report 264-6, University of Kansas Center for Research, Inc., Lawrence, Kansas, August 1975.

Cihlar, J., F.T. Ulaby, and R. Mueller, "Soil Moisture Detection from Radar Imagery," RSL Technical Report 264-4, University of Kansas Center for Research, Inc., Lawrence, Kansas, June 1975.

Idso, S.B., T.J. Schmugge, R.D. Jackson, and R.J. Reginato, "The Utility of Surface Temperature Measurements for the Remote Sensing of Surface Soil Water Status," *J. Geophys. Res.*, **80**, 1975, pp. 3044-3049.

Jackson, R.D., "Diurnal Changes in Soil Water Content During Drying," in *Field Soil Water Regime*, Soil Soc. of Am., Madison, Wisconsin, 1973, pp. 37-51.

Newton, R.W. and W.R. McClellan, "Permittivity of Soils at L-Band," Technical Report No. 58, Remote Sensing Center, Texas A&M University, June 1975.

Poe, G., A. Stogryn, and A.T. Edgerton, "Determination of Soil Moisture Content Using Microwave Radiometry," Final Report 1648 FR-1, DOC Contract 0-35239, Aerojet-General Corp. Microwave Division, El Monte, California, 1971.

Schmugge, T., P. Gloersen, T. Wilheit, and F. Geiger, "Remote Sensing of Soil Moisture With Microwave Radiometers," *J. Geophys. Res.*, **79**, 1974, p. 317.

APPENDIX A
PHOENIX GROUND TRUTH MAPS FOR THE APRIL 1974 FLIGHT MISSION

(Prepared under Contract NAS 9-12200 by Lockheed Electronics Company, Inc., Aerospace Systems Division, Houston, Texas.)

The following legend is applicable to the ground truth maps.

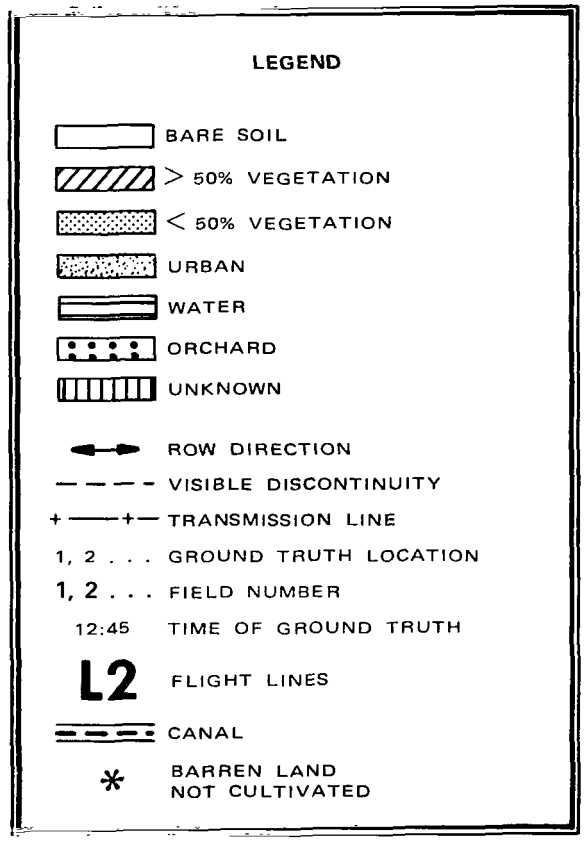

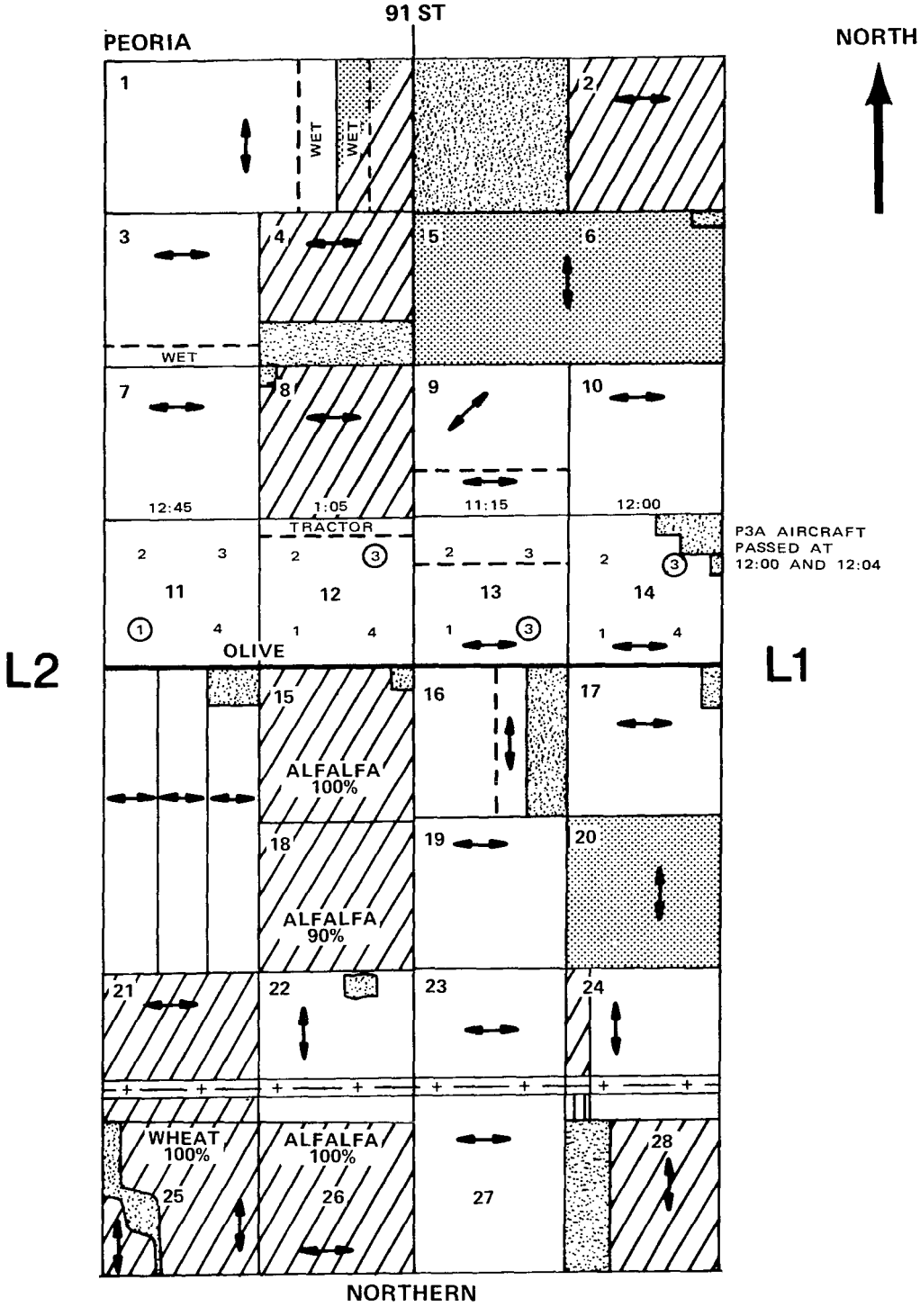
91 ST
PEORIA
NORTH
WET
WET
WET
TRACTOR
12:45
1:05
11:15
12:00
P3A AIRCRAFT
PASSED AT
12:00 AND 12:04
OLIVE
L2
L1
ALFALFA
100%
ALFALFA
90%
WHEAT
100%
ALFALFA
100%
NORTHERN

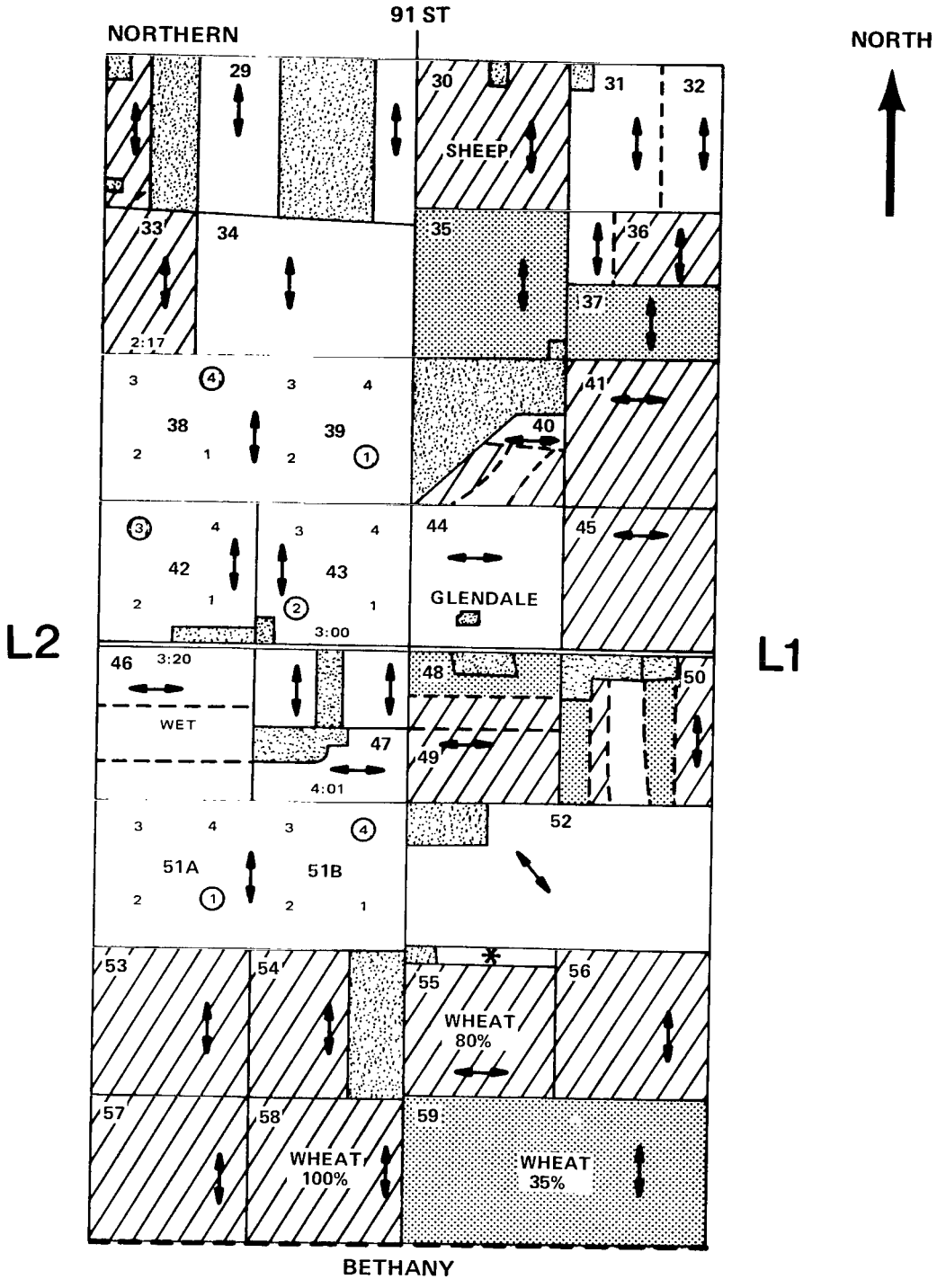
NORTHERN
91 ST
NORTH
29
30
31
32
SHEEP
33
34
35
36
37
2:17
3
4
38
39
40
41
2
1
42
43
44
45
GLENDALE
3:00
L2
L1
46
3:20
WET
47
48
49
50
4:01
51A
51B
52
53
54
55
56
WHEAT
80%
57
58
59
WHEAT
100%
WHEAT
35%
BETHANY

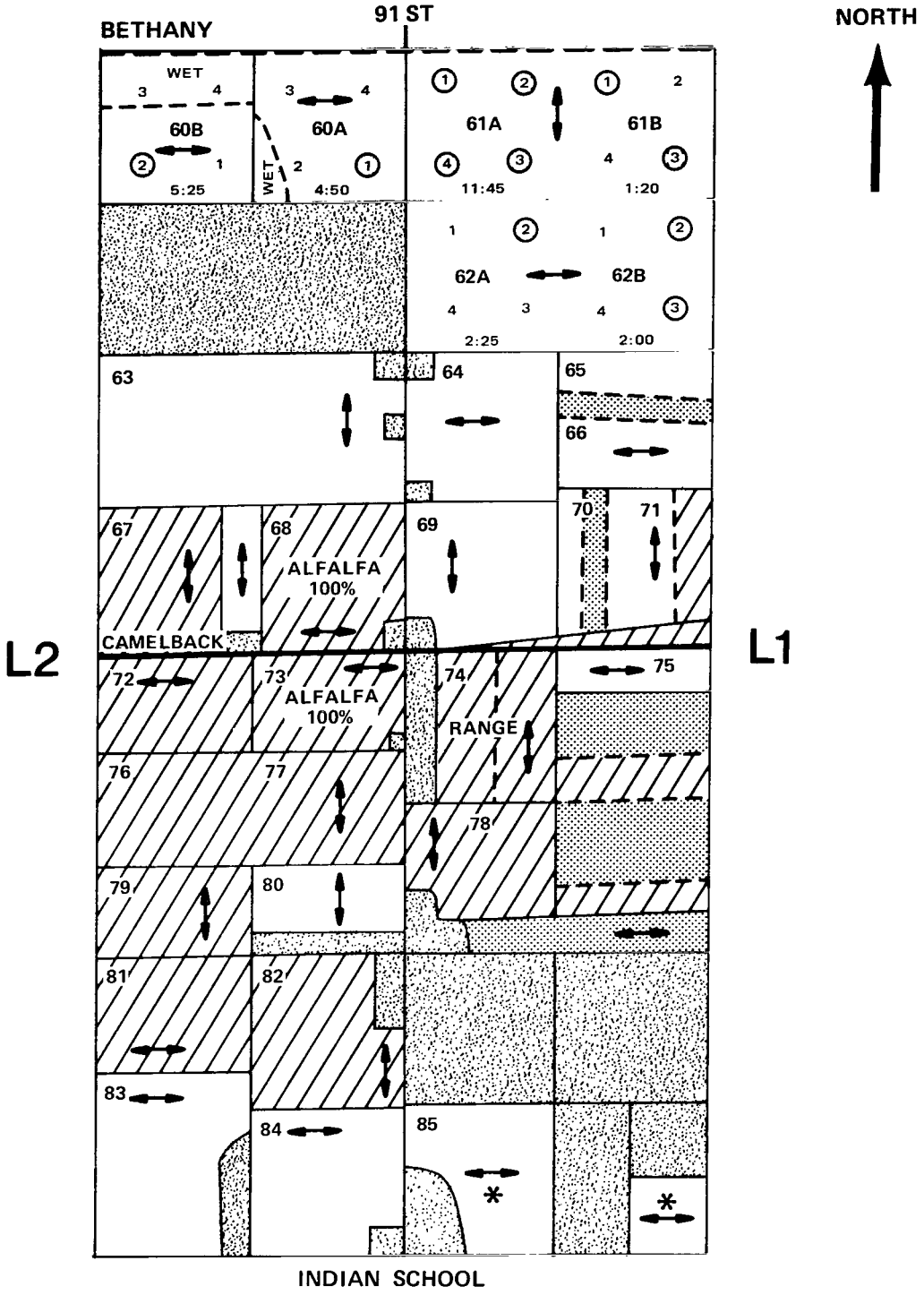
BETHANY
91 ST
NORTH
WET
60B
5:25
60A
WET
4:50
61A
11:45
61B
1:20
62A
2:25
62B
2:00
63
64
65
66
67
68
ALFALFA
100%
69
70
71
CAMELBACK
L2
L1
72
73
ALFALFA
100%
74
RANGE
75
76
77
78
79
80
81
82
83
84
85
INDIAN SCHOOL

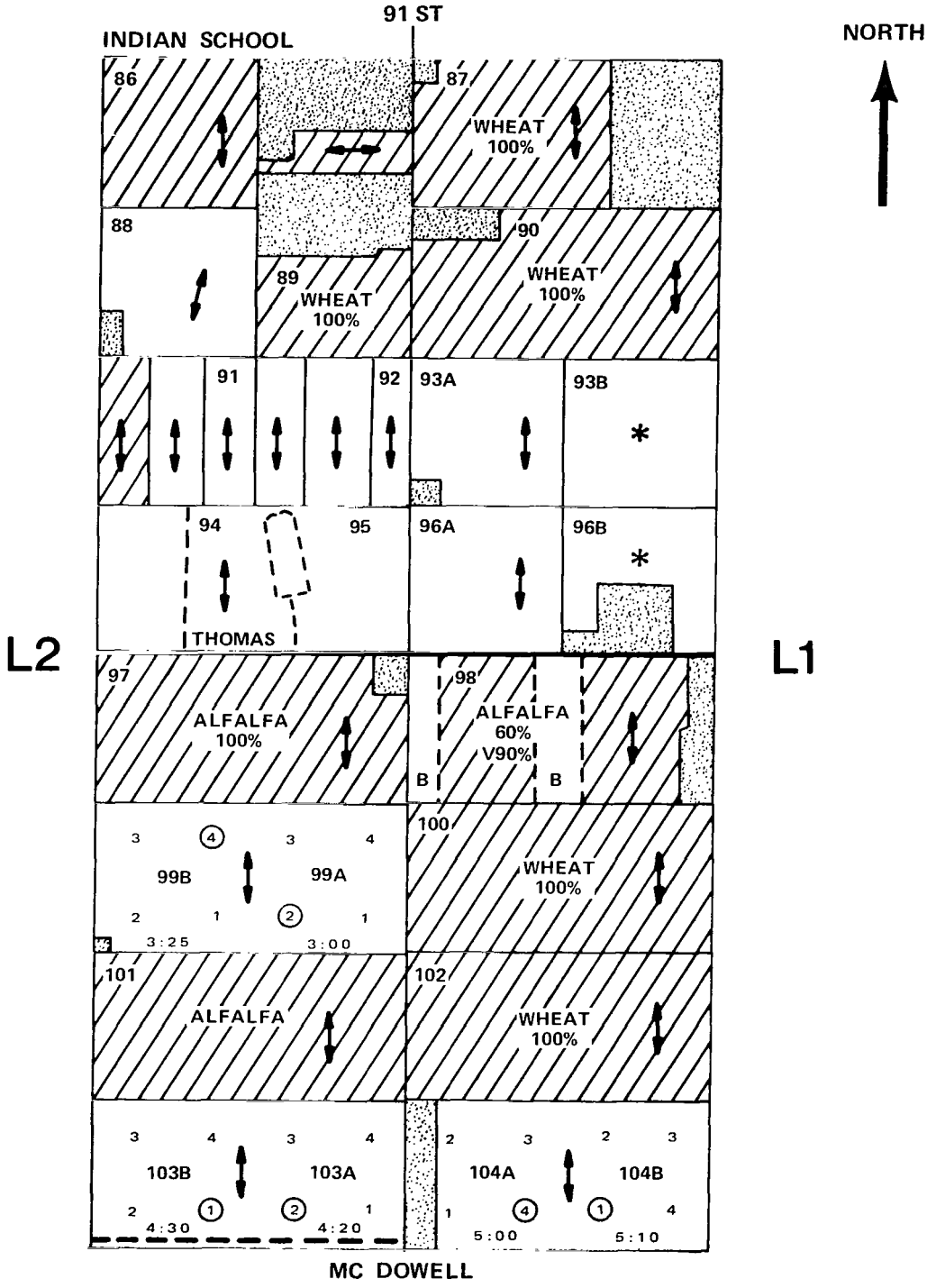
91 ST
INDIAN SCHOOL
NORTH
86
87
WHEAT
100%
88
90
89
WHEAT
100%
WHEAT
100%
91
92
93A
93B
*
94
95
96A
96B
*
THOMAS
L2
L1
97
ALFALFA
100%
98
ALFALFA
60%
V90%
B
B
100
3
4
3
4
99B
99A
WHEAT
100%
2
1
2
1
3:25
3:00
101
102
ALFALFA
WHEAT
100%
3
4
3
4
2
3
2
3
103B
103A
104A
104B
2
1
2
1
1
4
1
4
4:30
4:20
5:00
5:10
MC DOWELL

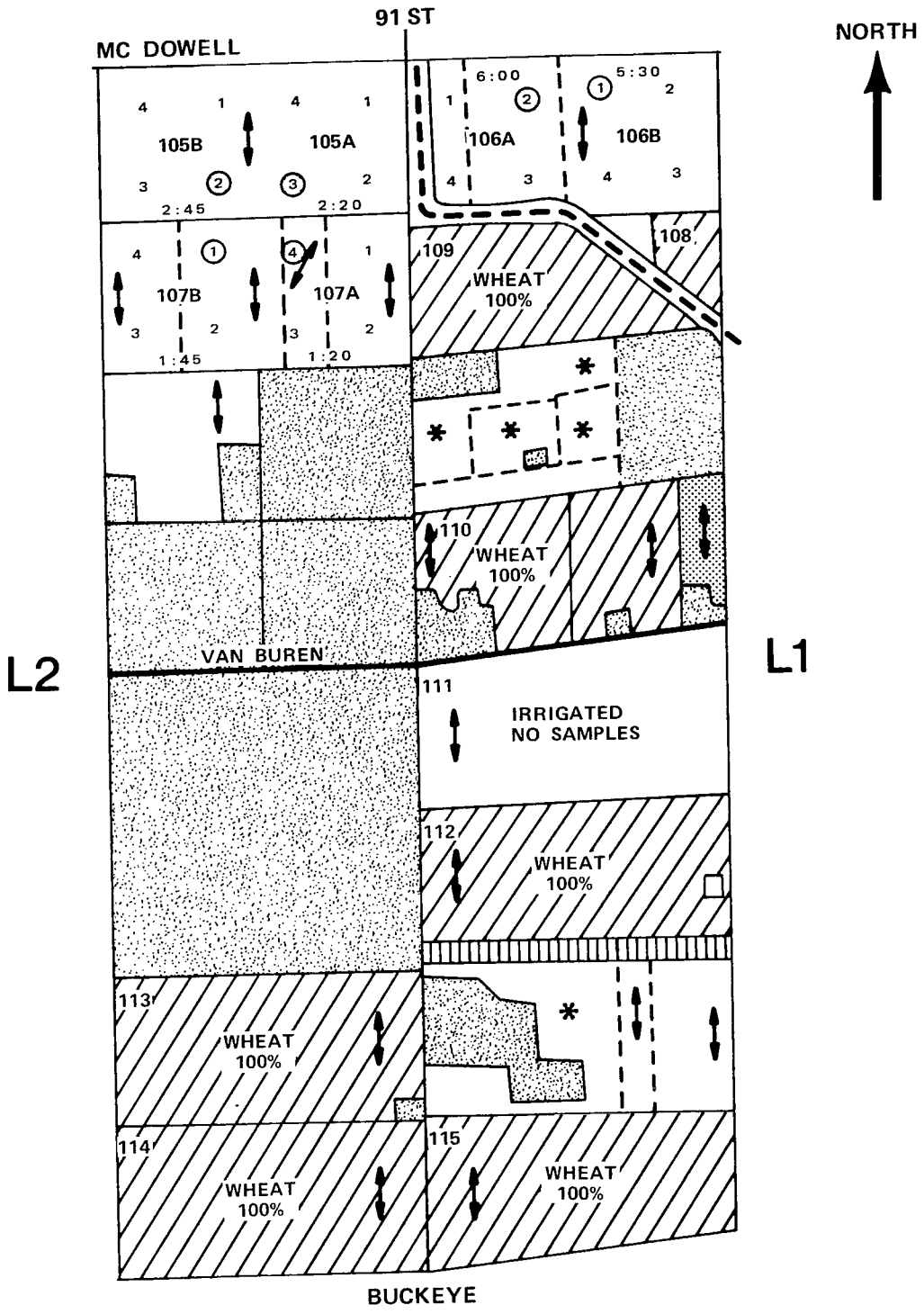
91 ST
MC DOWELL
NORTH
105B
105A
106A
106B
107B
107A
108
109
WHEAT
100%
110
WHEAT
100%
VAN BUREN
L2
L1
111
IRRIGATED
NO SAMPLES
112
WHEAT
100%
113
WHEAT
100%
114
WHEAT
100%
115
WHEAT
100%
BUCKEYE

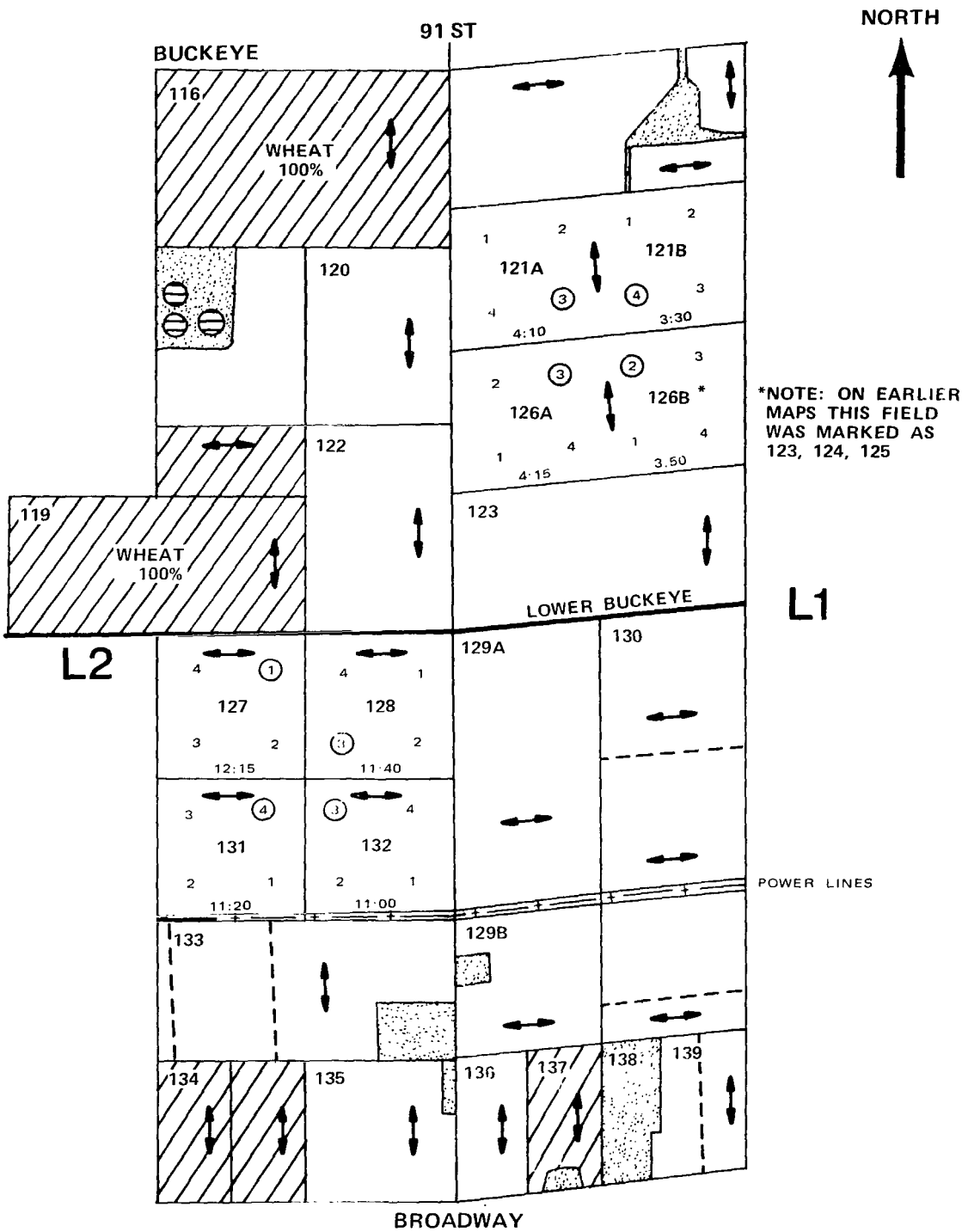

*NOTE: ON EARLIER MAPS THIS FIELD WAS MARKED AS 123, 124, 125

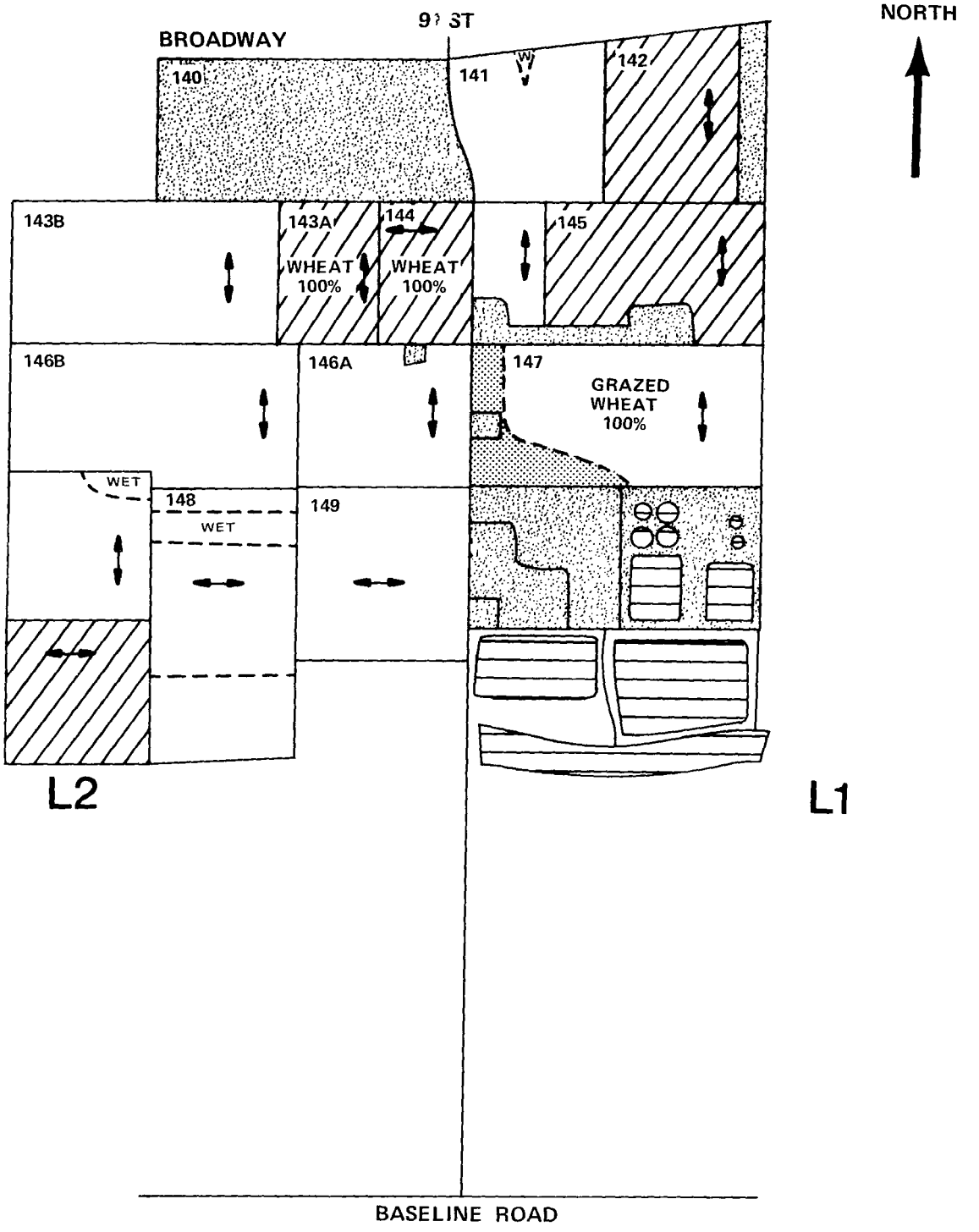
NORTH
BROADWAY
9? ST
140
141
142
143B
143A
144
145
WHEAT
100%
WHEAT
100%
146B
146A
147
GRAZED
WHEAT
100%
WET
148
WET
149
L2
L1
BASELINE ROAD

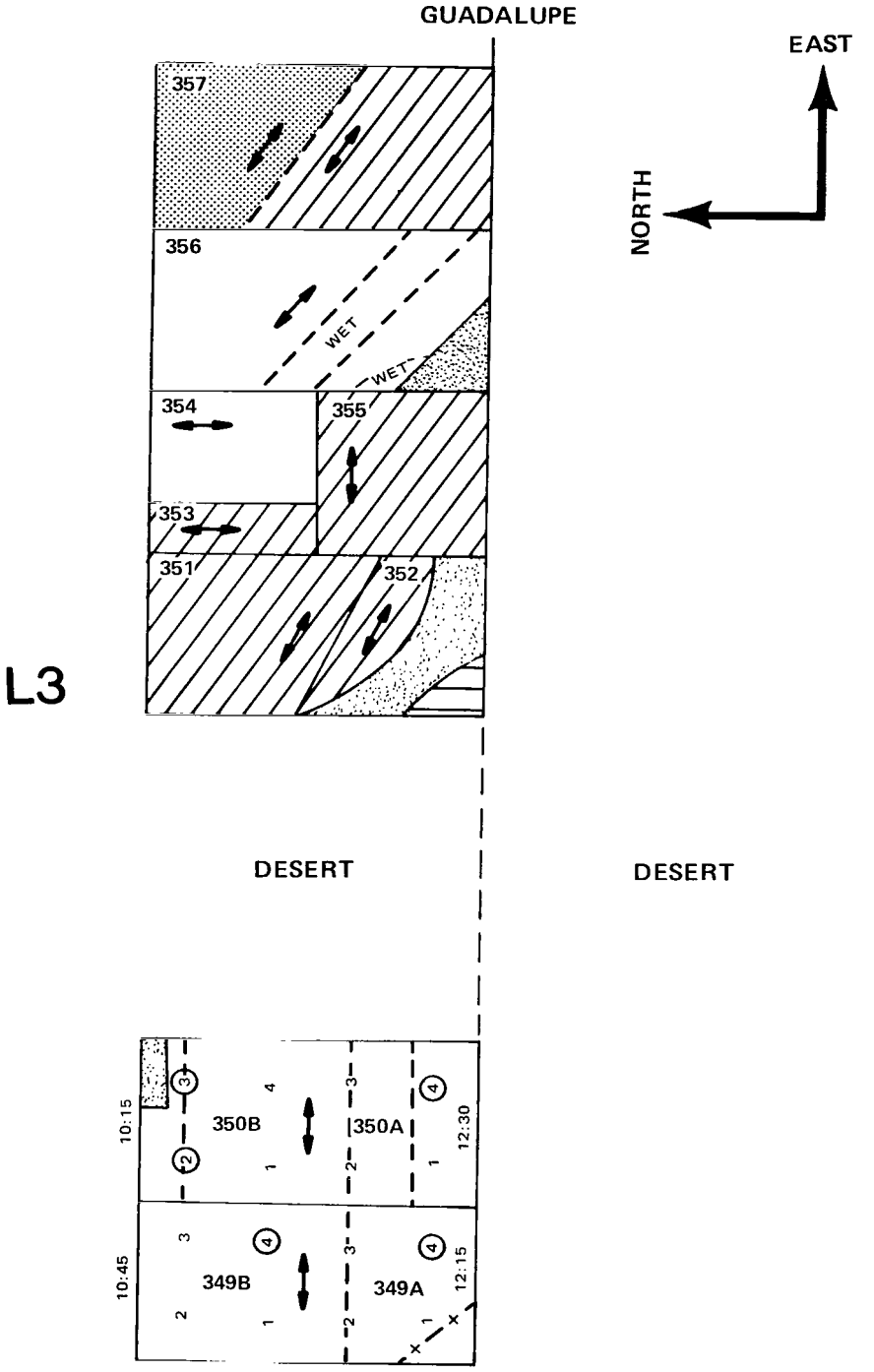
GUADALUPE
EAST
NORTH
357
356
WET
WET
354
355
353
351
352
L3
DESERT
DESERT
10:15
350B
350A
12:30
10:45
349B
349A
12:15

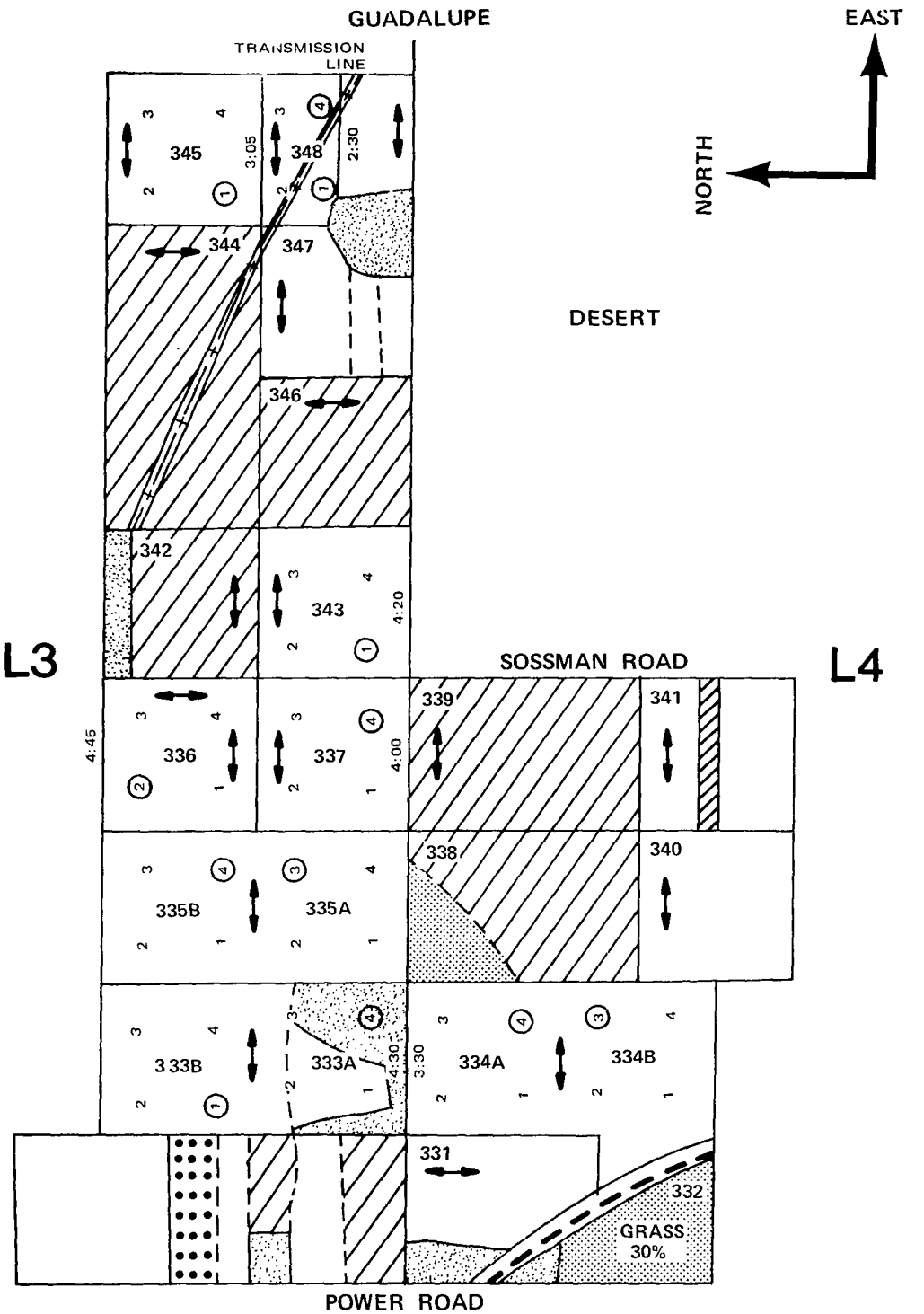
GUADALUPE
EAST
TRANSMISSION LINE
NORTH
345
348
344
347
DESERT
346
342
343
L3
SOSSMAN ROAD
L4
339
341
336
337
338
340
335B
335A
333B
333A
334A
334B
331
332
GRASS 30%
POWER ROAD

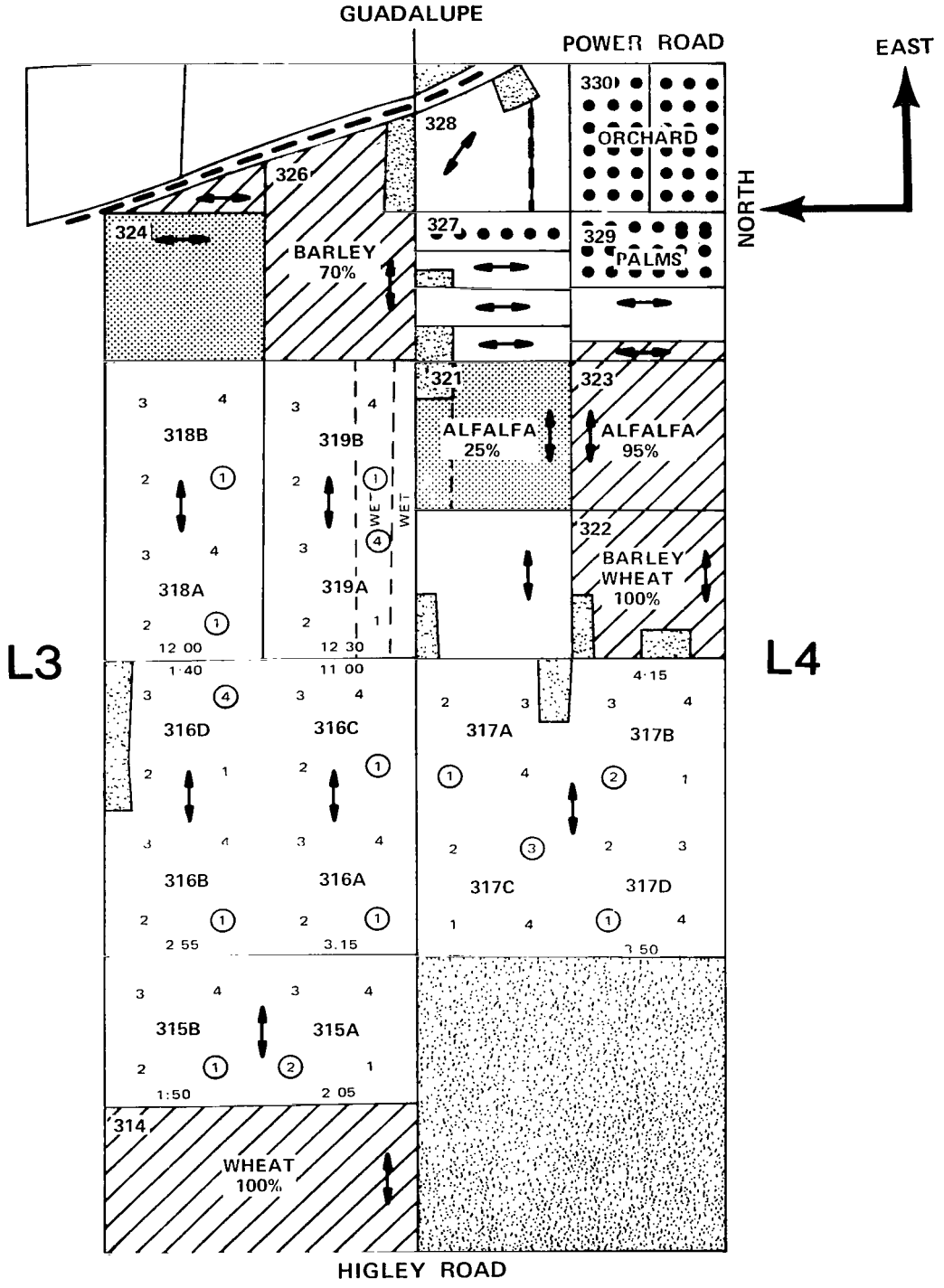
GUADALUPE
POWER ROAD
EAST
NORTH
330
ORCHARD
328
326
327
329
PALMS
324
BARLEY
70%
321
323
ALFALFA
25%
ALFALFA
95%
322
BARLEY
WHEAT
100%
318B
319B
318A
319A
WET
12 00
1 40
12 30
11 00
4 15
L3
L4
316D
316C
317A
317B
316B
316A
317C
317D
2 55
3.15
315B
315A
1:50
2 05
314
WHEAT
100%
HIGLEY ROAD

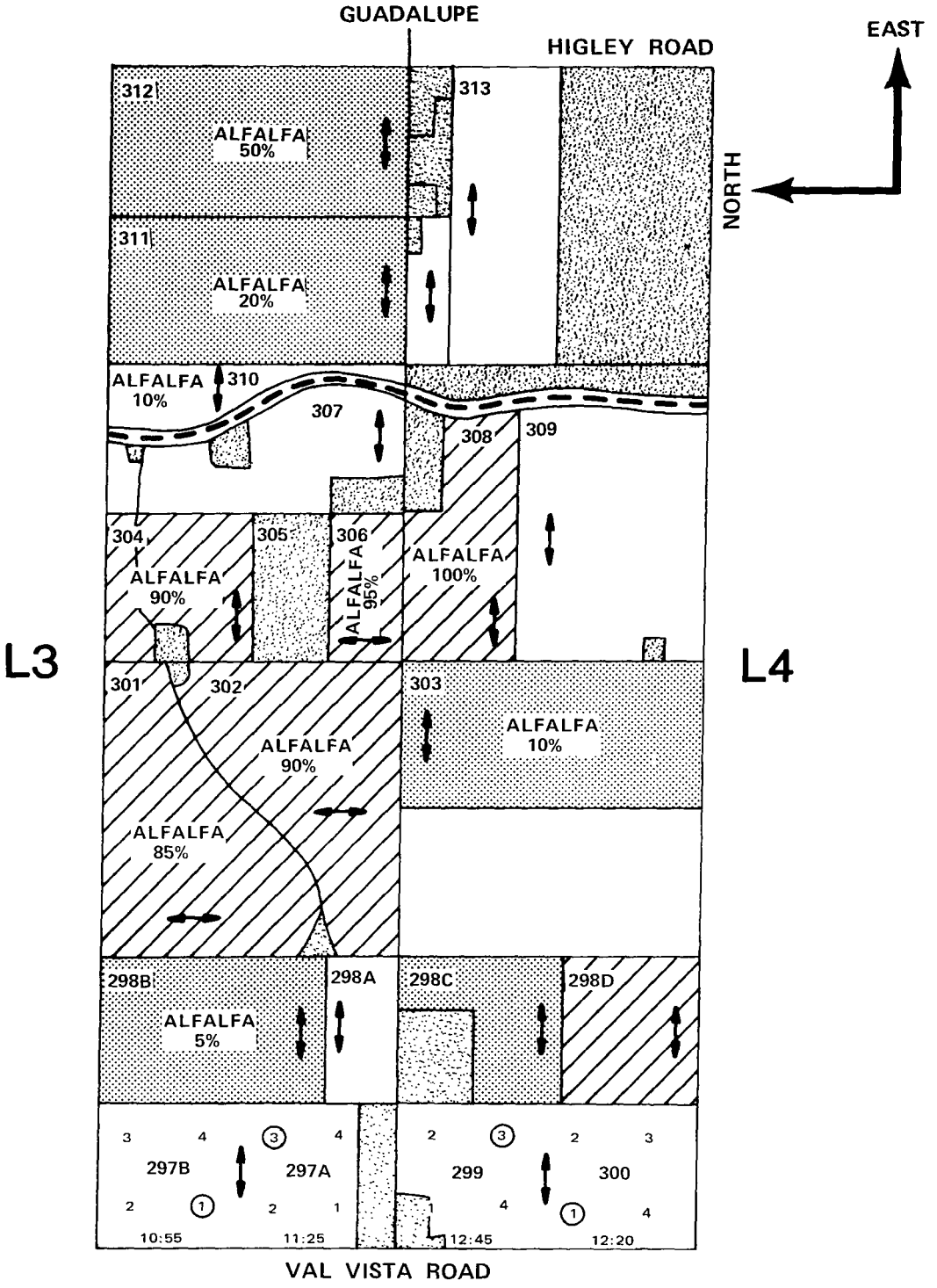
GUADALUPE
HIGLEY ROAD
EAST
NORTH
312
ALFALFA 50%
313
311
ALFALFA 20%
ALFALFA 10%
310
307
308
309
304
305
306
ALFALFA 90%
ALFALFA 95%
ALFALFA 100%
L3
L4
301
302
303
ALFALFA 90%
ALFALFA 10%
ALFALFA 85%
298B
298A
298C
298D
ALFALFA 5%
297B
297A
299
300
10:55
11:25
12:45
12:20
VAL VISTA ROAD

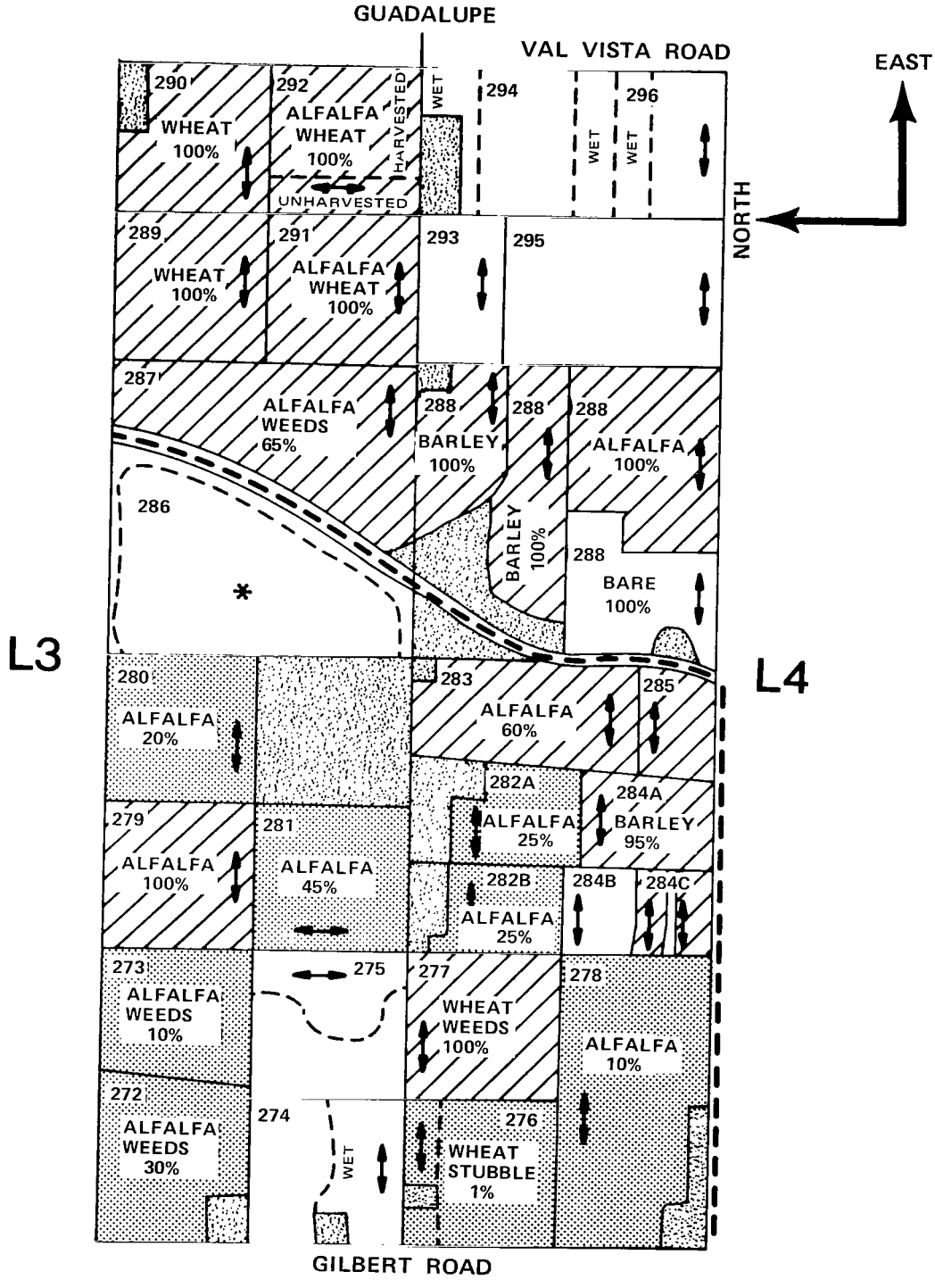
GUADALUPE
VAL VISTA ROAD
EAST
NORTH
290
WHEAT
100%
292
ALFALFA
WHEAT
100%
HARVESTED
UNHARVESTED
WET
294
WET
WET
296
289
WHEAT
100%
291
ALFALFA
WHEAT
100%
293
295
287
ALFALFA
WEEDS
65%
288
BARLEY
100%
288
288
ALFALFA
100%
286
*
BARLEY
100%
288
BARE
100%
L3
L4
280
ALFALFA
20%
283
ALFALFA
60%
285
282A
ALFALFA
25%
284A
BARLEY
95%
279
ALFALFA
100%
281
ALFALFA
45%
282B
ALFALFA
25%
284B
284C
273
ALFALFA
WEEDS
10%
275
277
WHEAT
WEEDS
100%
278
ALFALFA
10%
272
ALFALFA
WEEDS
30%
274
WET
276
WHEAT
STUBBLE
1%
GILBERT ROAD

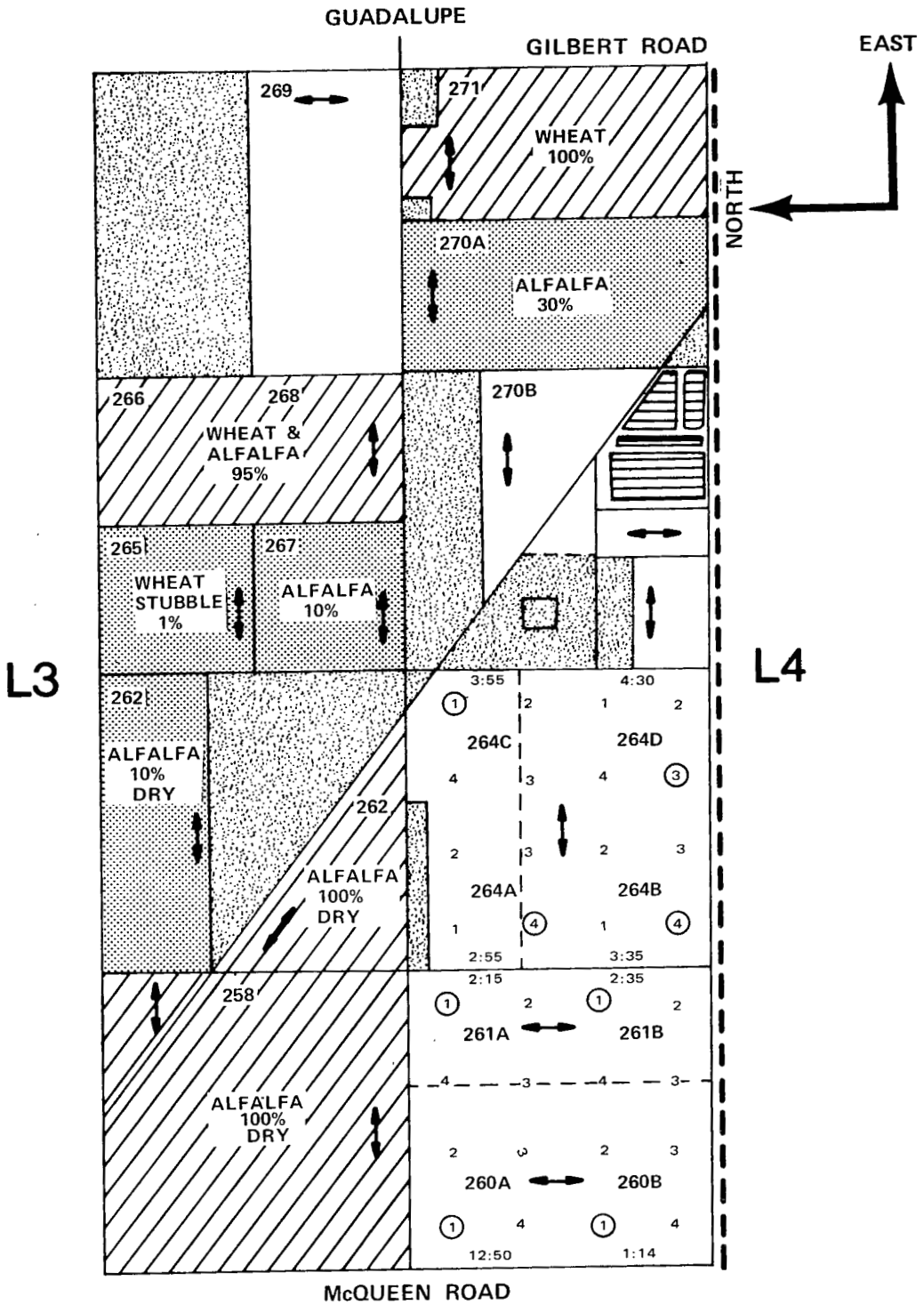
GUADALUPE
GILBERT ROAD
EAST
NORTH
269
271
WHEAT
100%
270A
ALFALFA
30%
266
268
WHEAT &
ALFALFA
95%
270B
265
WHEAT
STUBBLE
1%
267
ALFALFA
10%
L3
L4
262
ALFALFA
10%
DRY
262
ALFALFA
100%
DRY
3:55
4:30
264C
264D
264A
264B
2:55
3:35
2:15
2:35
258
261A
261B
ALFALFA
100%
DRY
260A
260B
12:50
1:14
McQUEEN ROAD

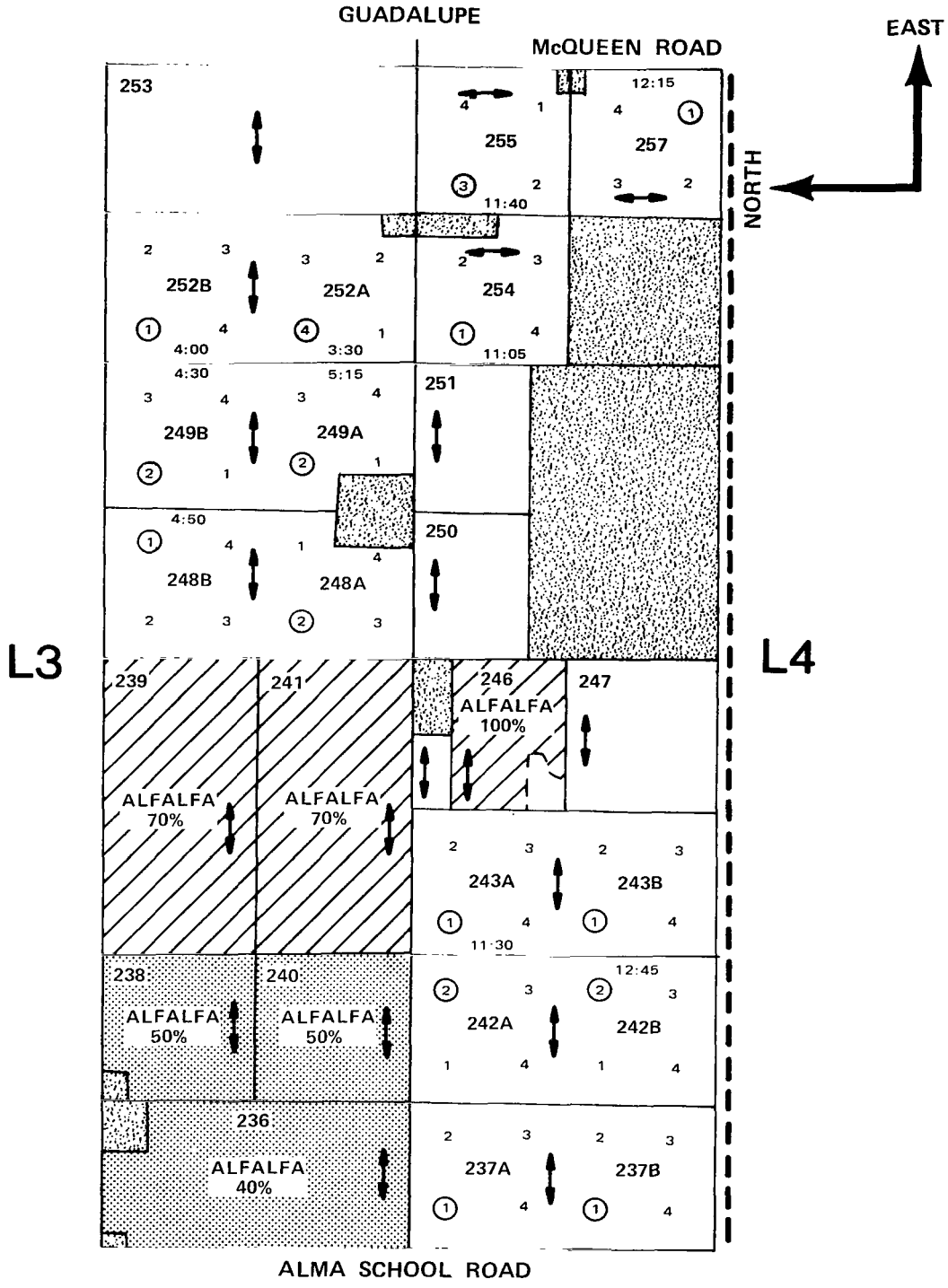
GUADALUPE
McQUEEN ROAD
EAST
NORTH
253
255
257
252B
252A
254
251
249B
249A
250
248B
248A
L3
L4
239
241
246
ALFALFA
100%
247
ALFALFA
70%
ALFALFA
70%
243A
243B
11:30
238
240
12:45
ALFALFA
50%
ALFALFA
50%
242A
242B
236
ALFALFA
40%
237A
237B
ALMA SCHOOL ROAD

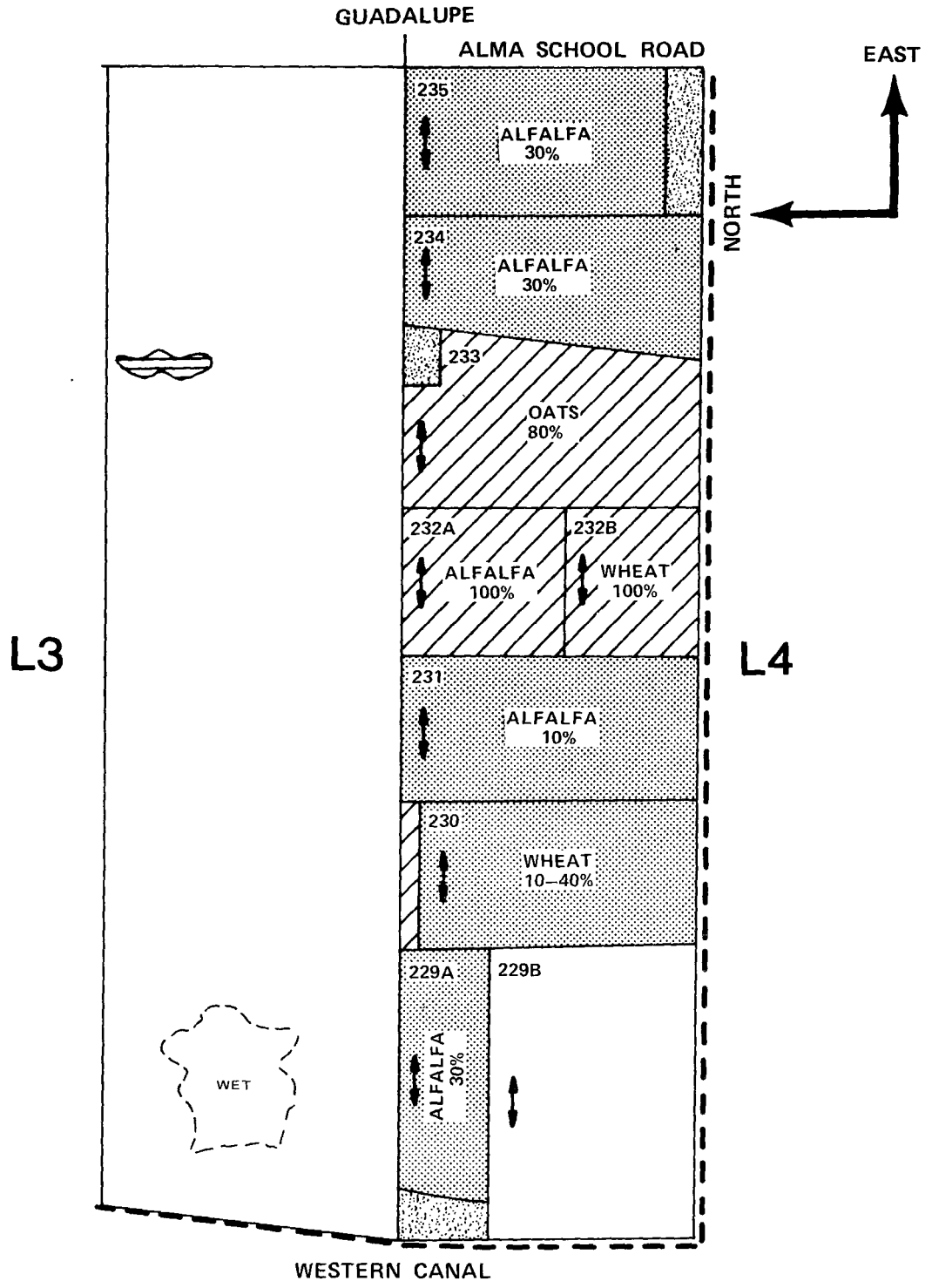
GUADALUPE
ALMA SCHOOL ROAD
EAST
NORTH
235
ALFALFA
30%
234
ALFALFA
30%
233
OATS
80%
232A
ALFALFA
100%
232B
WHEAT
100%
L3
L4
231
ALFALFA
10%
230
WHEAT
10–40%
229A
229B
ALFALFA
30%
WET
WESTERN CANAL

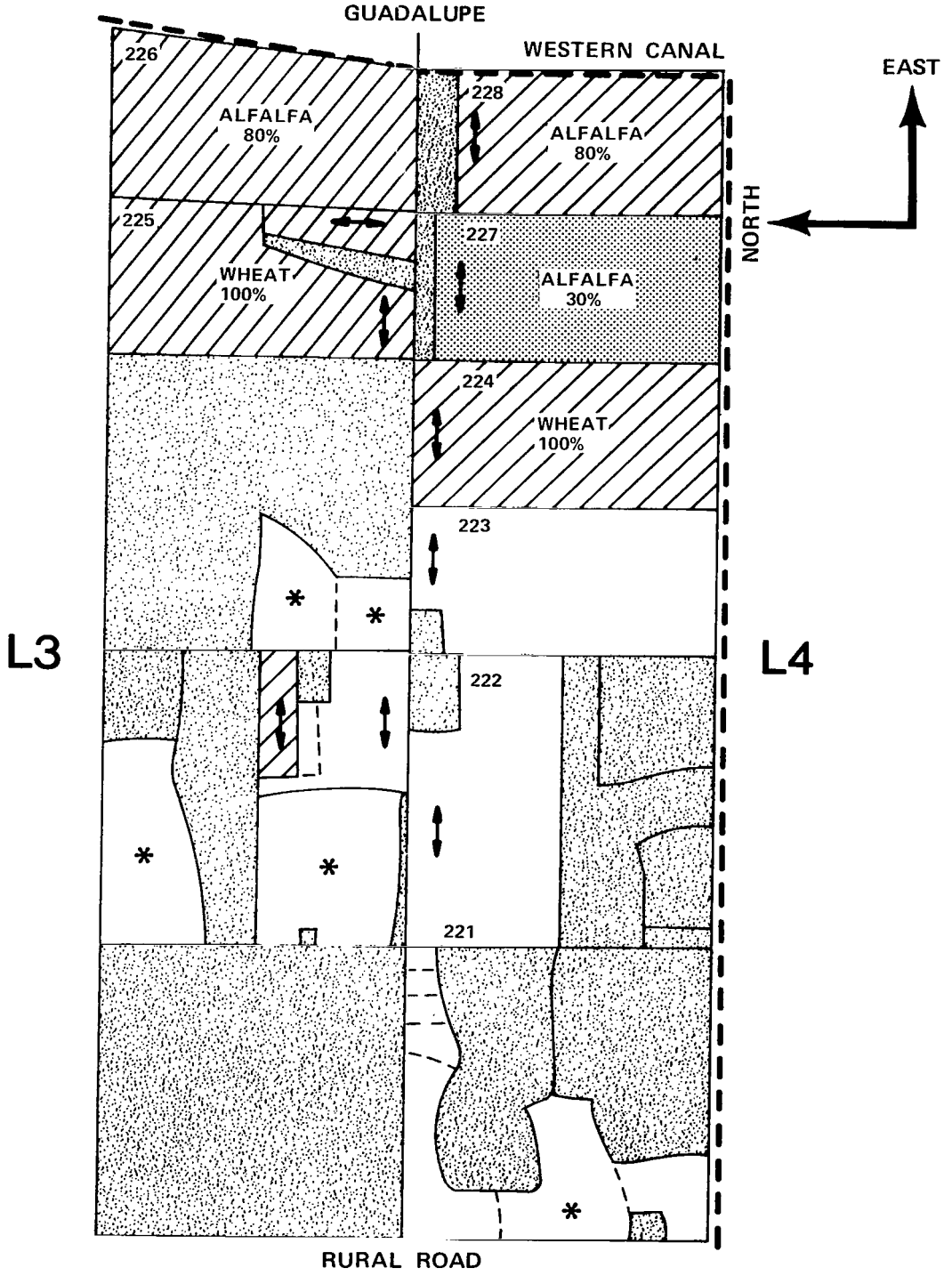
GUADALUPE
WESTERN CANAL
EAST
NORTH
226
228
ALFALFA
80%
ALFALFA
80%
225
227
WHEAT
100%
ALFALFA
30%
224
WHEAT
100%
223
L3
L4
222
221
RURAL ROAD

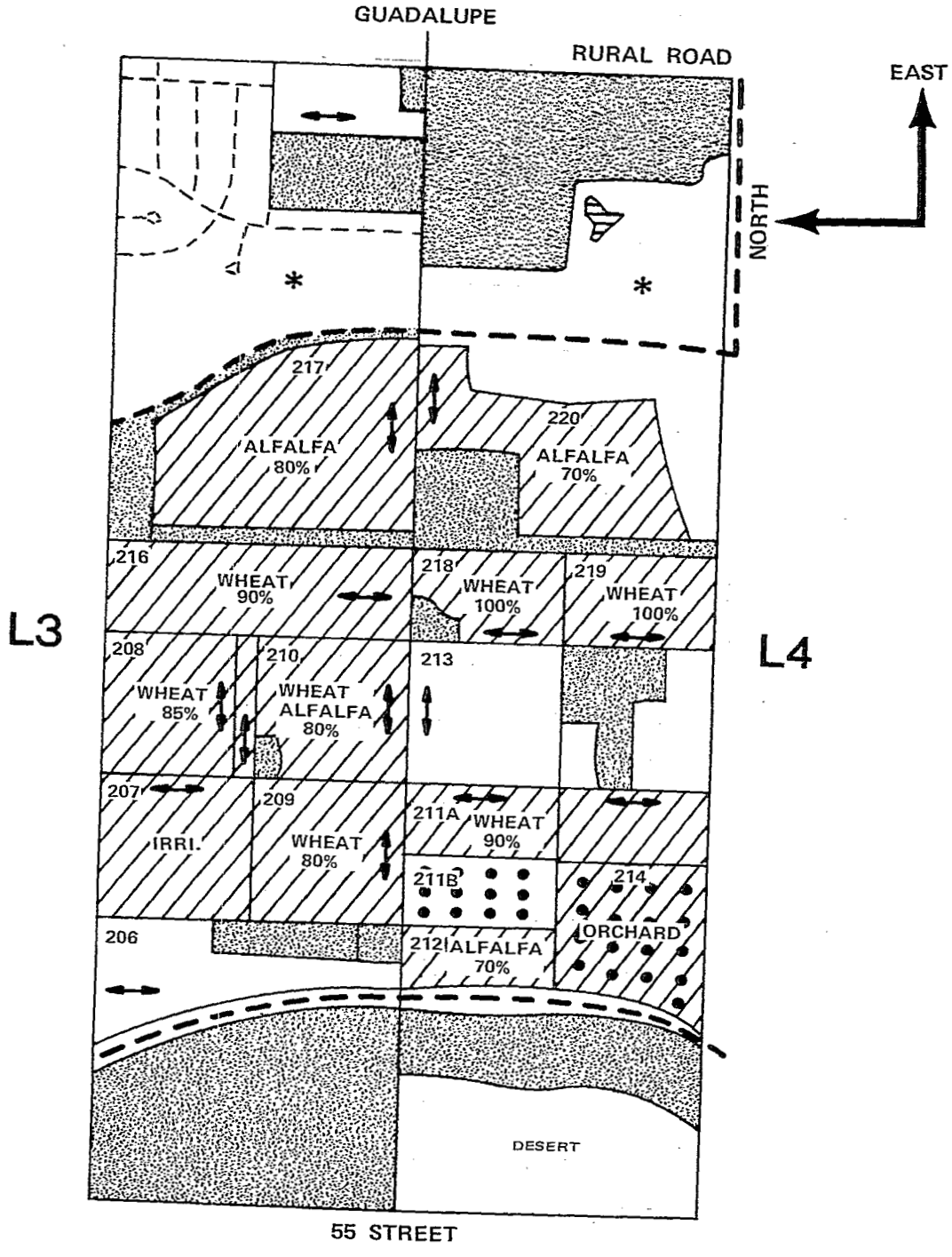
GUADALUPE
RURAL ROAD
EAST
NORTH
L3
L4
217
ALFALFA
80%
220
ALFALFA
70%
216
WHEAT
90%
218
WHEAT
100%
219
WHEAT
100%
208
WHEAT
85%
210
WHEAT
ALFALFA
80%
213
207
IRRI.
209
WHEAT
80%
211A
WHEAT
90%
211B
214
ORCHARD
206
212
ALFALFA
70%
DESERT
55 STREET

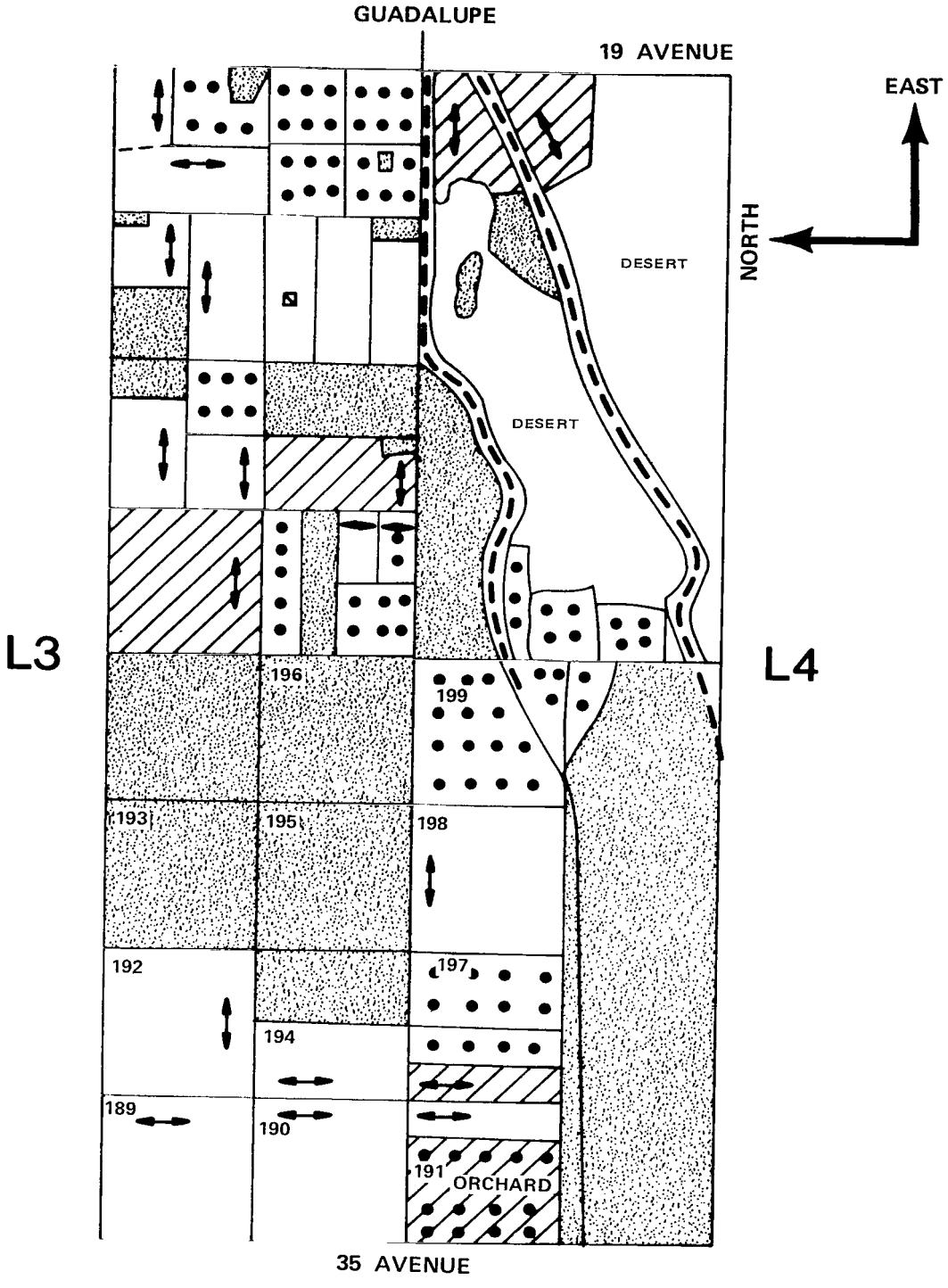
GUADALUPE
19 AVENUE
EAST
NORTH
DESERT
DESERT
L3
L4
196
199
193
195
198
192
197
194
189
190
191
ORCHARD
35 AVENUE

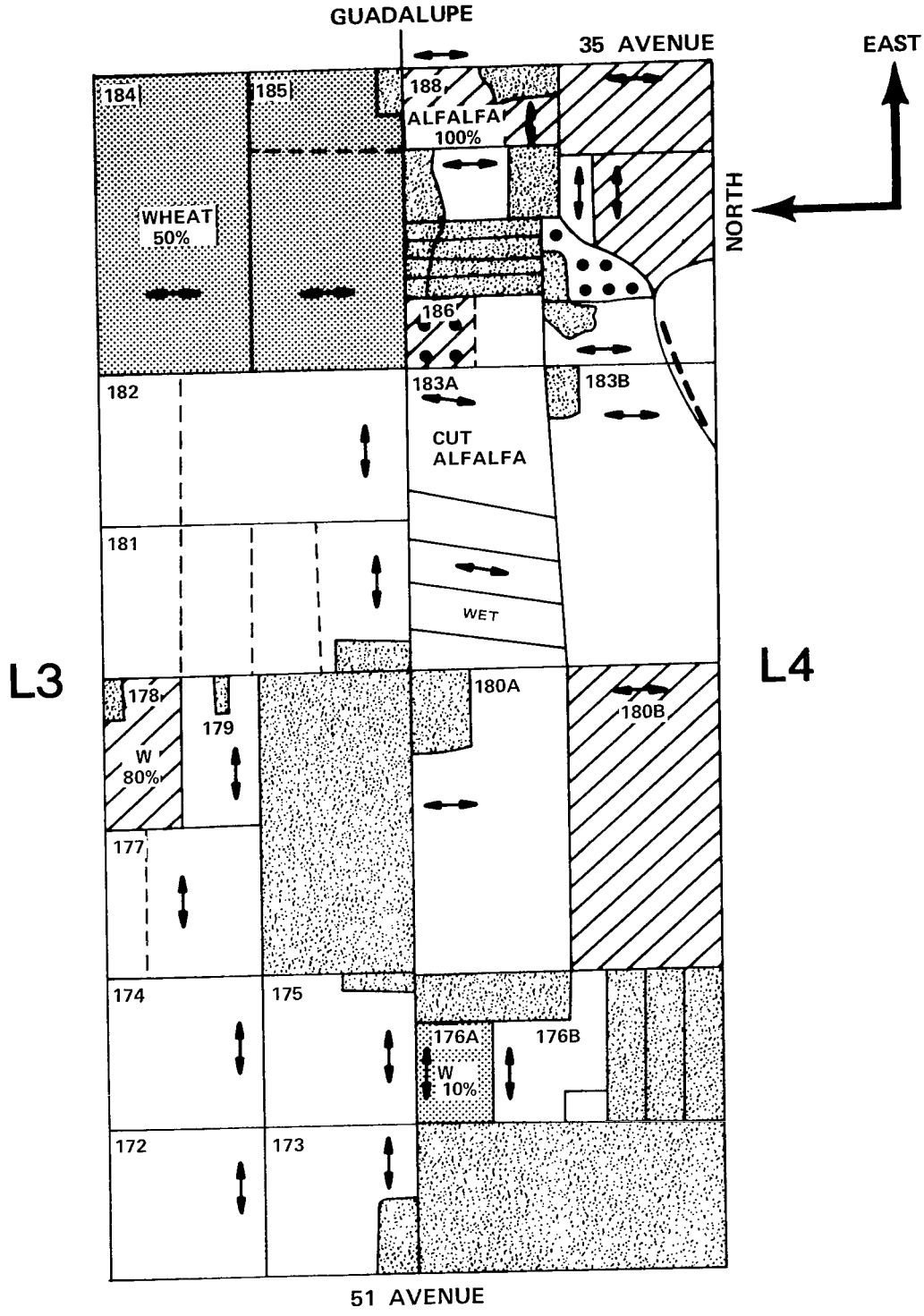
GUADALUPE
35 AVENUE
EAST
NORTH
184
185
188
ALFALFA
100%
WHEAT
50%
186
182
183A
183B
CUT
ALFALFA
181
WET
L3
L4
178
W
80%
179
180A
180B
177
174
175
176A
176B
W
10%
172
173
51 AVENUE

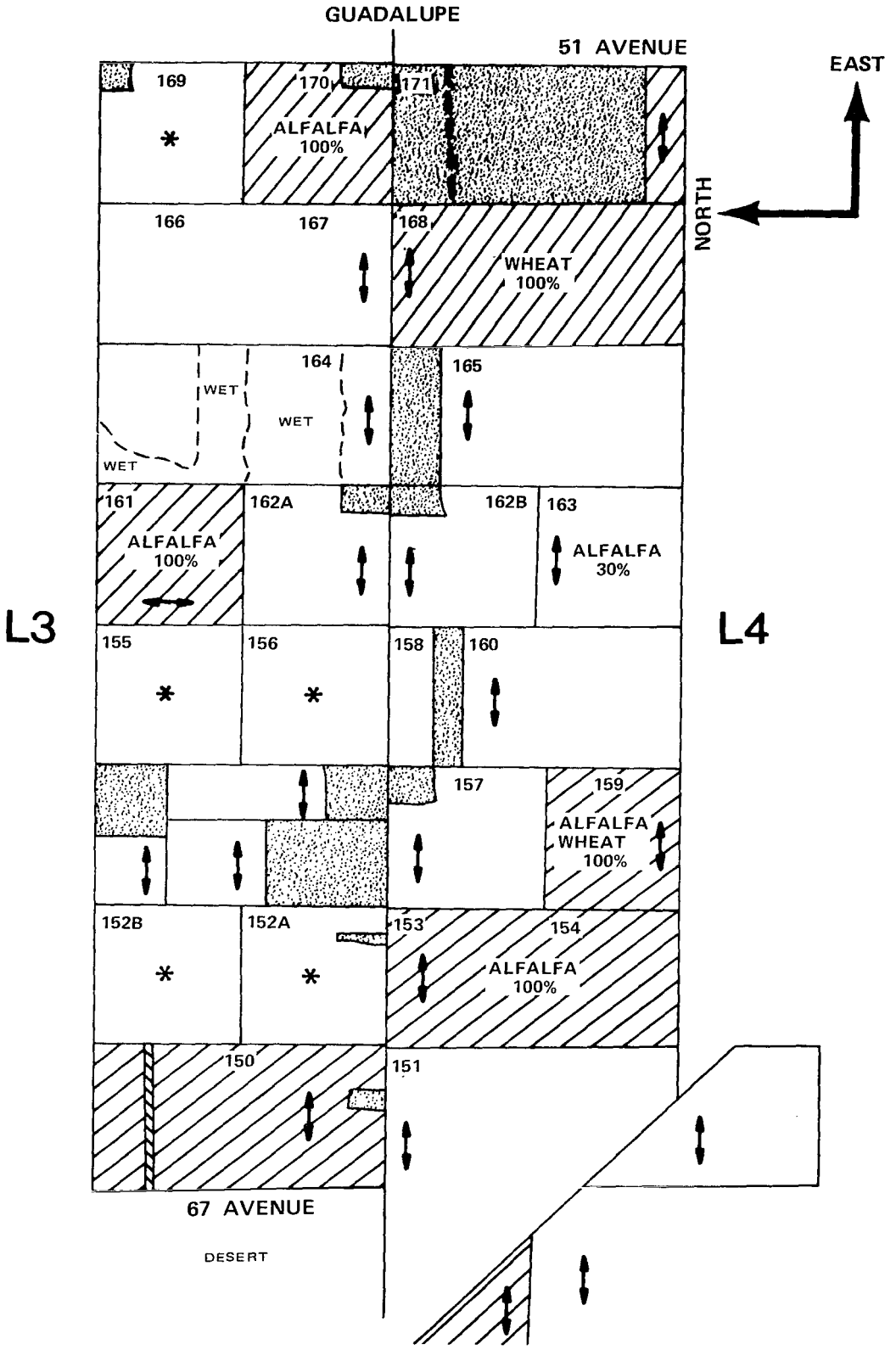
GUADALUPE
51 AVENUE
EAST
NORTH
169
170
171
ALFALFA
100%
166
167
168
WHEAT
100%
164
165
WET
WET
WET
161
162A
162B
163
ALFALFA
100%
ALFALFA
30%
L3
L4
155
156
158
160
157
159
ALFALFA
WHEAT
100%
152B
152A
153
154
ALFALFA
100%
150
151
67 AVENUE
DESERT

APPENDIX B
SURFACE MEASUREMENTS

This appendix is a summary of the soil moisture sampling procedures used in the soil moisture experiment and contains an estimate of the confidence that should be placed in those procedures.

Prior experience indicated that gravimetric soil moisture samples representing several layers of near-surface soils would be required. At each sample point, a separate gravimetric sample was collected representing the 0- to 1-cm, the 1- to 2-cm, 2- to 5-cm, 5- to 9-cm, and the 9- to 15-cm layers of soil. An attempt was made to collect sufficient soil at each depth to provide a dry weight of at least 80 g. This was not always attained for the top two layers. Samples were sealed in plastic bags and marked with the appropriate sample location and depth increment. The samples were weighed, dried in an oven at 378 K (105°C), and weighed again. The percent of soil moisture is determined by dividing the difference of these two weights by the dry weight. Drying in the oven at the standard temperature, 378 K (105°C), resulted in the cracking of some bags and the loss of soil from the sample, thus some fields where samples were collected are not reported.

SELECTION OF FIELDS

The study area selected was in the vicinity of Phoenix, Arizona. Selection of the area was based on the availability of large numbers of bare fields located on reasonably uniform surface soils where irrigation practices would normally provide a wide variation in soil moisture. The area was also used in prior studies,* and extensive data were compiled documenting the physical properties of the soils. Some of the variability expected in the soil moisture samples can be better understood by reviewing the field selection procedures and the results of soil moisture sampling prior to the flight experiment.

Aerial photography from previous NASA aircraft missions were used to detect some fields that exhibited differences in soils that would influence differences in drying rate, particularly in the first 2 cm on the surface. Such fields are undesirable for a study of this nature, because it is physically impossible to collect enough samples to adequately define the mean soil moisture. Trips were made to examine the tillage practices and soil conditions in each field that was considered. Based on our surface observations, aerial photography, and soil map information, a decision to use or to avoid the available bare fields was made.

*Schmugge, T., P. Gloersen, T. Wilheit, and F. Geiger, "Remote Sensing of Soil Moisture With Microwave Radiometers," *J. Geophys. Res.*, 79, 1974, p. 317.

SOIL MOISTURE VARIABILITY

Soil moisture measurements for prior experiments concerned with the near-surface soils offer some opportunity to understand the variance in soil moisture that can be expected. It was found that fields of intermediate soil moisture content can be expected to exhibit greater variance than fields that are extremely wet or dry.

The drying rate of surface soil layers is influenced by the physical characteristics of the profile. Also, soil textures (that is, fractions of sand, silt, and clay making up the soil) have a major influence on drying rates. However, by selection of fields with relatively uniform soils, differences in drying due to the difference in soil fractions should be a minor factor within each field used for this experiment.

More localized differences in drying rates can be due to variations in local relief and to differences in density either resulting from tillage or irrigation practices. Such local conditions can rarely be contolled. The variance exhibited in samples collected for this experiment are most likely as small as could be expected in fields with listed rows exposed to several hours of sunshine. The tops of the furrows in the Phoenix area are usually loose, friable soil that receives moisture by lateral and vertical (capillary) flow, while the bottoms are more compact soil that is flooded in the common furrow irrigation practice.

One field (260B) was sampled at 36 locations to gain some understanding of the reliability of sets of four samples per field. The field was irrigated for two days prior to sampling with an application of approximately 25 cm of water (1 acre-foot of water per acre). Samples were collected representing each depth increment (0 to 1 cm, 1 to 2 cm, 2 to 5 cm, 5 to 9 cm, 9 to 15 cm) from both the top and the bottom of the furrow at each of the 36 sample points.

Figures 1a and 1b of the text are illustrations showing contours of the percentage of soil moisture in the depth increment (0 to 1 cm) for the top and the bottom of furrows, respectively. These figures indicate that drying rates vary considerably within a field. Highs and lows in the two plots do not coincide; therefore, it appears that the elevation at the sample point on top of the furrow has little influence in this particular field.

The coefficient of variation (standard deviation ÷ mean) was calculated for the 36 measurements at each depth increment and are listed in table B-1. The standard deviations for the near-surface increments were large, and the mean soil moisture was low when compared to measurements from deeper soil layers. The results illustrate how the coefficient of variation decreases with depth for the particular conditions found in field 260B during the midday time period. A coefficient of variation less than 0.15 would be most desirable for soil moisture measurements to be used as verification for microwave calibration. This requirement might be met by arranging flights and field sampling in the early morning hours. The decreased evaporation during the night permits stabilization of moisture in the near-surface soil by capillary movement. Until the surface has acquired heat supplied by the sun, evaporation rates will be lower than the rate at midday.

To obtain an estimate of the accuracy obtained by using four data points to represent a field, the 36 samples from field 260B were divided into four groups of nine locations. One hundred stratified random samples consisting of one sample from each quarter of the field were selected. The means of the stratified random samples were compared to the overall mean of the field. This distribution of means from the samples of the four locations were not normally distributed about the field mean. The distribution of the 100 means for each depth increment indicates that there is a 90 percent chance that a sample from four locations in the field will fall within the following limits given in table B-1.

Table B-1

Coefficient of Variation			Limits of Confidence	
Soil Layer cm	Top of Furrow	Bottom of Furrow	Field Mean (%)	Limits (%)
0-1	0.27	0.36	15.8	-2.9 to +3.5
1-2	0.18	0.30	18.4	-2.6 to +3.1
2-5	0.14	0.11	21.8	-2.5 to +2.4
5-9	0.11	0.09	23.1	-1.8 to +2.6
9-15	0.07	0.10	23.9	-1.5 to +1.7

As expected, the surface layers have the largest uncertainty, and these limits should be considered the estimates of the surface measurement accuracy.

TEXTURE ANALYSIS

A texture analysis was performed on the soil from each field, and the results are given in the above tables. The textures are expressed as the weight percent, that is, sand, silt, or clay. Sand particles are defined by the size range of 2 to 0.05 mm, silt particles by the range from 0.05 to 0.002 mm, and clay particles are less than 0.002 mm. This texture information is necessary for determining the moisture holding characteristics of the soil. In particular, this texture information was used to make estimates of the field capacity of the soil (that is, the amount of water remaining in the soil 2 to 3 days after an irrigation) and the wilting point (WP) of the soil (that is, the point at which plants can no longer absorb water from the soil). The relationships used to calculate these quantities in percent soil moisture are:

$$WP = 7.2 - 0.07 \times \text{sand} + 0.24 \times \text{clay}$$

and

$$FC = 25.1 - 0.21 \times \text{sand} + 0.22 \times \text{clay}$$

where sand and clay are their respective fractions expressed in percent. These relations were obtained by performing a multiple regression analysis using data for 100 soils for which the texture and moisture characteristics were known.

"The aeronautical and space activities of the United States shall be conducted so as to contribute . . . to the expansion of human knowledge of phenomena in the atmosphere and space. The Administration shall provide for the widest practicable and appropriate dissemination of information concerning its activities and the results thereof."

—NATIONAL AERONAUTICS AND SPACE ACT OF 1958

NASA SCIENTIFIC AND TECHNICAL PUBLICATIONS

TECHNICAL REPORTS: Scientific and technical information considered important, complete, and a lasting contribution to existing knowledge.

TECHNICAL NOTES: Information less broad in scope but nevertheless of importance as a contribution to existing knowledge.

TECHNICAL MEMORANDUMS: Information receiving limited distribution because of preliminary data, security classification, or other reasons. Also includes conference proceedings with either limited or unlimited distribution.

CONTRACTOR REPORTS: Scientific and technical information generated under a NASA contract or grant and considered an important contribution to existing knowledge.

TECHNICAL TRANSLATIONS: Information published in a foreign language considered to merit NASA distribution in English.

SPECIAL PUBLICATIONS: Information derived from or of value to NASA activities. Publications include final reports of major projects, monographs, data compilations, handbooks, sourcebooks, and special bibliographies.

TECHNOLOGY UTILIZATION PUBLICATIONS: Information on technology used by NASA that may be of particular interest in commercial and other non-aerospace applications. Publications include Tech Briefs, Technology Utilization Reports and Technology Surveys.

Details on the availability of these publications may be obtained from:

SCIENTIFIC AND TECHNICAL INFORMATION OFFICE

NATIONAL AERONAUTICS AND SPACE ADMINISTRATION

Washington, D.C. 20546